ABSTRACT

DAVIS, OLGHA BASSAM. Refining an Elastic Constitutive Equation to Predict Pressure Distributions for Normotensive and Hypertensive Aortas. (Under the direction of Dr. Brooke N. Steele).

Constitutive equations are used to mathematically represent arterial wall mechanical properties. Accurate vascular wall models are crucial for providing acceptable simulation results of arterial blood pressure (ABP) wave propagation. An important consideration when determining the constitutive equation is the effect of ABP on vessel wall compliance; the tendency of the arteries to expand and contract in response to ABP. The goal of this work is to model the compliance of normotensive and hypertensive aortas to mathematically describe vessel distensibility. While large vessels exhibit a viscoelastic characteristic, the determination of pure elastic modulus is a reasonable first approximation. The arterial stiffness is expressed in terms of pressure-strain elastic modulus (E_o) and stress-strain Young's modulus (E). The elastic modulus may be computed directly from gradients of pressure and diameter measurements. In addition to strain and pressure, Young's modulus requires the cross-sectional area of the vessel wall to compute stress. Wall thickness (h) and vessel undeformed radius (r_o) vary due to numerous factors including, but not limited to age and morbidity. In this work, three methods are used to approximate Eh/r_o , compute the corresponding pressure for a given diameter, and compare the computed pressure to experimental data. The first method uses an empirical model by Olufsen to approximate Eh/r_o with a decaying exponential function of r_o and a constant offset k_3 . This k_3 term is used to compute pressure using an elastic constitutive equation. For the second method, it is noted that for large vessels ($r_o > 0.6cm$), including the aorta, the previous empirical method

relies only on the constant offset term. Therefore, this k_3 parameter is optimized for normotensive and hypertensive data using the Nelder-Mead method. Lastly, the third method incorporates patient-specific pulse pressure and diastolic radii, which are readily available from clinical diagnostic data, with an approximation of the pulsatile change in radius (Δr) as a percentage of r_o . This percentage is different for normotensive and hypertensive models. All three methods are applied to data found in the literature including human and canine normotensive aortas and human hypertensive aortas. Based on this work, using patient-specific approach in estimating the pressure distributions for corresponding diameter measurements appears to be the best to approximate the normotensive pressure distribution for a given patient's diameter measurements and pulse pressure readings. However, no conclusive evidence was found to determine a best-fit model to approximate pressure distribution for hypertensive subjects.

Refining an Elastic Constitutive Equation to Predict Pressure Distributions for Normotensive and Hypertensive Aortas

by
Olgha Bassam Davis

A thesis submitted to the Graduate Faculty of
North Carolina State University
in partial fulfillment of the
requirements for the degree of
Master of Science

Biomedical Engineering

Raleigh, NC

2008

APPROVED BY:

_____	_____
Dr. Mansoor A. Haider	Dr. Caterina M. Gallippi
_____	_____
Dr. David S. Lalush	Dr. Brooke N. Steele Chair of Advisory Committee

BIOGRAPHY

As an undergraduate student at Boston University, I participated in various research projects as early as freshman year. In early 1995, I started working at the Sensors and Actuators Laboratory under the supervision of Dr. Johannes Smits. One of my first tasks was to lead a laboratory portion of a freshman class in Silicon Motors in a clean room environment. Shortly after, I was involved in a fascinating research project that was supported by Jet Propulsion Laboratory of NASA, where I led a group of undergraduate and graduate students in designing and building a micro-mechanical gas pumps for gas chromatographic equipment that was planned to be flown on the mission to Mars in year 2001. In addition to the NASA research project, I was closely involved in designing and developing beam locators using silicon chips according to specification from Raytheon, a leader in defense technology development. My final research project at Dr. Johannes Smits' Laboratory was to successfully build Silicon-Gold electrode cavities in arrays for mass-spectrometry of DNA for Biomedical applications.

After graduating with a Bachelor's Degree in Biomedical Engineering from Boston University, in May 1998, I worked for the MathWorks Inc., a privately held software company. My first position at the MathWorks was as a technical support engineer, where I assisted users in the scientific, mathematics and engineering fields while efficiently trouble-shooting real world problems such as installation, programming, printing, and manipulating data in the MATLAB® software environment. In October of 1999, I was promoted to a training engineer position. As a result, I have developed, facilitated and instructed complex courses to users of the MathWorks products. Many of the customers that I interacted with

worked for top companies such as General Motors, Ford, DaimlerChrysler, Caterpillar, Eaton, NASA and MIT. Working with these bright engineers has enhanced my people skills and ignited my desire to teach. By the time I departed the MathWorks in July of 2005, I was considered one of their leading and most requested training engineers who has helped shape the future direction of this company.

In August of 2005, I started my graduate degree at the joint program at North Carolina State University and the University of North Carolina at Chapel Hill. Currently, I am involved in research projects that include theoretical and hands-on approaches in developing a surgical planning device that can be used to advance cardiovascular discipline. This work completes my Master's degree in Biomedical Engineering under the supervision of Dr. Brooke Steele.

ACKNOWLEDGEMENTS

I would like to acknowledge my supporting husband, Jarvis and my beautiful daughter, Dalya, you both are my inspiration in completing this degree.

I would like to acknowledge my advisor, Dr. Brooke N. Steele, for her advice and assistance in working towards earning this degree.

I would like to thank the rest of my committee, Dr. Mansoor Haider, Dr. Caterina Gallippi, and Dr. David Lalush for their guidance.

TABLE OF CONTENTS

LIST OF TABLES

LIST OF FIGURES

Chapter 1. Introduction

1.1 Motivation

According to the American Heart Association, Cardiovascular Disease (CVD) has been the number one killer disease in the United State since 1919 and the medical costs associated with its treatment are estimated to rise to $2.8 trillion by 2011. CVD takes decades to develop, and manifests in many different ways including focal accumulation of plaques, and both focal and global changes in the arterial properties due to mechanically-driven forces [1]. A better understanding of normal and abnormal arterial mechanics is vital in enhancing diagnostic techniques, understanding vascular disease progression, and refining surgical planning tools.

Scientific literatures show strong indications that the mechanics of healthy arteries behave like viscoelastic solid materials [1-3]. As the arterial wall mechanical properties change with disease and age, the blood vessels become stiffer and respond differently to stress, strain, and shear mechanical forces. As arteries become stiffer, they lose their viscoelastic properties and behave like an elastic material. Although the number of technologies that measure arterial wall shear stress and strain are few, researchers have developed mathematical models to describe the mechanics of healthy and unhealthy vessels. Some of the common models are elastic pressure-diameter model, pseudoelastic strain energy functions, and the viscoelastic model [1, 4, 5]. While large vessels exhibit viscoelastic behavior, invasive techniques are required to measure simultaneous pressure and diameter data for loading and unloading. Linear elastic models rely on absolute pressure and diameter

gradients, allowing non-invasive cuff pressure to be used with diameter gradients measured with non-invasive imaging techniques. In this study; elastic pressure-diameter constitutive equations are used to model the mechanical properties of normotensive and hypertensive aortas.

1.2 Specific Aims

The goal of this research is to characterize normotensive and hypertensive aortic wall mechanics using a 1-D constitutive equation. The outcome of this project address the first steps necessary to develop a parameter mapping of material properties of large arteries and produce more accurate predictions of blood pressure. The specific aim of this work is to:

Specific Aim 1: Identify a mapping between mathematical representation of the arterial wall properties and their measurable mechanical properties. The working hypothesis for this aim is that vessel properties will be characterized based on hemodynamic, environment and size characterize the viscoelastic behavior of the arteries. This can be achieved by developing a linear 1-D model and mapping its parameters to the arterial wall responses due to hysteresis. We expect that these parameters will have different mathematical values that map to the various mechanical properties of the arterial wall.

Specific Aim 2: Validate the derived elastic model with *in vivo* human and canine experiments. In this specific aim, we will provide a comprehensive assessment of unexposed arterial wall stiffness based on measured radius and pressure. We will validate the derived constitutive model with measured data for various vessel segments including the

thoracic aorta, ascending aorta, and the abdominal aorta from normal and hypertensive humans and normal canine subjects.

Chapter 2. Background and Significance

2.1 Overview

The arterial mechanical properties are an important determination of hemodynamics. Larger arteries, such as aortas, are distended rapidly during systole and then relax during diastole. Because of these dimensional changes, the viscoelastic properties of the walls of these large vessels are a factor in determining instantaneous pressure. When the arteries are pressurized (deformed) they are subjected to distention in all directions. In vivo, arterial motion occurs predominantly in the circumferential direction with very little movement in the longitudinal direction. In this study, experimental data and analytical methods are limited to circumferential deformations.

2.2 Physiology of the Arteries

Blood vessel mechanical properties are strongly influenced by their location in the body and the elasticity of their walls [1-4, 6]. The wall's elasticity is altered by concentrations and structural collections of elastin and collagen fibers.

Arteries can be organized into two groups: elastic and muscular groups. The elastic arteries are more distensible, larger in size, and positioned near the heart, while the muscular arteries are less distensible, smaller in size, and are located away from the heart, near the arterioles [2]. The aorta, aorta branches, and the iliac are some examples of elastic arteries. While the coronary, the cerebral, the femoral, and the renal arteries are some examples of the muscular arteries. Figure 1 shows the systemic circulation and the artery locations

throughout the body.

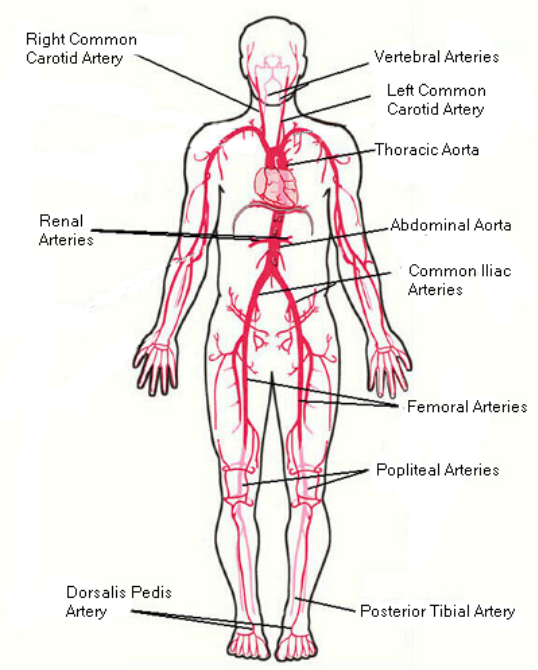

Figure 1 Systemic Circulation Arteries
This image was modified from an image found at www.medicalook.com.

In this study, we treat the vessel wall as a homogenous material and consider the mechanical properties of its layers under quantitative parameters: the undeformed radius (r_o), the wall thickness (h), the radius oscillation (Δr), and the Young's modulus (E). Ideally, the undeformed (unpressurized) arterial radius can only be measured ex-vivo. However in vivo, r_o is approximated as the diastolic radius, smallest measureable radii. Although vascular wall structure and thickness variations have been noted along the aortic length, the vessel wall is generally assumed to deform and to have a uniform wall thickness (h) of approximately 10-15% of the undeformed vessel radius (r_o) [1, 7, 8]. The radius gradient (Δr) is the total difference between the systolic and diastolic radii. The radius oscillation

(Δr) of unexposed healthy human and canine aortas is approximated as 9-12% of the undeformed vessel radius (r_o) [9, 10]. Strain is the fractional increase in dimension (i.e. radius or length), while stress is the force (i.e. internal pressure) per unit area exerted by the tissue at each level of strain. The Young's modulus (E) is a measure of arterial stiffness and is the ratio of stress and strain.

In addition to modeling healthy aortas, this study also attempts to model diseased (hypertensive) aortas. Hypertension is a form of vascular disease that is characterized by a patient with chronic high blood pressure. As a result of hypertension, the aortic wall remodels, losing its elastin fibers (increasing the vessel's stiffness). Simultaneously, the vessel wall stiffens and thickness due to the increased level of collagen [3, 11, 12].

2.3 Pressure-Strain Elastic Modulus (E_o) and Young's Modulus (E)

The mechanical property of any solid material is described using the modulus, a quantitative measurement that mathematically describes the material stiffness as the ratio of stress and strain. Arterial wall stiffness is normally expressed in terms of the pressure-strain elastic modulus (E_o) and the stress-strain Young's modulus (E). It is well-known that both moduli enlarge with age and hypertension to reflect the increase in the vessel wall stiffness. The elastic modulus is directly computed from systolic and diastolic measurements as follow:

$$E_o = \frac{(\Delta P) * (r_o)}{(\Delta r)} \tag{1.1}$$

The pressure pulse (ΔP) is defined as the difference between systolic pressure and diastolic pressure, and the pulsatile change in radius (Δr) is defined as the difference between systolic

radius (r_{max}) and diastolic radius (r_o). In this study, the pressure-strain elastic modulus (E_o) is computed directly from experimental data, using diastolic and systolic pressure and radius measurements for both normotensive and hypertensive aortic pressures.

The Young's modulus (E) can be derived using equation (1.12) that relates E to r_o and h. Note that in vivo r_o is approximated as the diastolic radius, the smallest measurable radius.

The vascular wall is made up of a combination of collagen, elastin fibers, and smooth muscle cells. Collagen is known to be the stiffest wall component with a Young's modulus of $10^8 - 10^9 g/s^2cm$ which is about two orders of magnitudes larger than the elastin component. The elastin Young's modulus ranges from $1 - 6x10^6 g/s^2cm$ while smooth muscle cell E ranges between $0.1 - 2.5x10^6 g/s^2cm$. It has been shown that E for a thoracic aorta of a healthy human is $4.0x10^6 g/s^2cm$ which falls in the range of elastin fibers and smooth muscle's moduli [7]. With aging and hypertension, the vessel stiffness approaches the stiffness of a rigid tube with E approximately equal to the collagen elastic modulus ($10^8 - 10^9 g/s^2cm$) which is much higher than the normotensive E of $4.0x10^6 g/s^2cm$ [7, 13].

2.4 Constitutive Equation

Constitutive equations can be used to model the mechanical properties of the arterial wall by characterizing the stress-strain relationship. The constitutive equation functional form choice depends on the mechanical behavior to be mathematically represented and the

availability of data to develop and validate the model. Vascular walls have been treated as pseudoelastic, viscoelastic, or pure elastic materials [1, 5]. A pseudoelastic model uses two separate equations to describe the loading and unloading characteristics of the material. Despite its simplicity to fit empirical dataset, a pseudoelastic model may yield an unrealistic prediction of the pressure-diameter loop since it is not easily translated into other datasets. In most invasive in vivo experiments, loading in one direction is generally accompanied by unloading in another, making a precise definition of pseudoelasticity a real challenge. Viscoelastic models include time-dependent responses and are useful for incorporating the viscoelastic behavior of large vessels (hysteresis, creep and stress relaxation). While large vessels exhibit viscoelastic behavior, invasive and costly techniques are required to measure simultaneous pressure and diameter data for loading and unloading per patient basis. Linear pure elastic models rely on absolute pressure and diameter gradients, allowing non-invasive cuff pressure to be used with diameter gradients measured with non-invasive imaging techniques.

In this study, we use an in vivo approach to derive the mechanical properties of healthy human, unhealthy human, and healthy canine specific vessels. Then, the arterial wall is modeled as an elastic material. An elastic material deforms due to applied force (internal blood pressure) and returns to its original undeformed state once this force is removed. Since we are analyzing the vessel in the body, we assume that the undeformed state is at diastole; the minimum amount of internal pressure is applied to the arterial wall. We assume that the arterial wall is a single homogeneous thin (with respect to the vessel radius) layer. Since it is a 1-D model, residual stresses are not accounted for and wall stresses are average values,

where $\sigma_{\phi\phi}$ represents the circumferential stress in the vessel wall.

Assuming an axially symmetric vessel, ABP causes loading and deformation of the arterial walls. This elastic deformation provides key characteristics of the mechanical properties of the blood vessels. The mechanical response of the blood vessel is time dependent, therefore temporal and spatial domains will be considered. The momentum equation for solid-state material, neglecting body and inertial forces is:

$$\nabla \bullet \sigma = 0\,, \tag{1.2}$$

in cylindrical coordinates ($\boldsymbol{r}, \phi, \boldsymbol{z}$), where σ is a vector of stresses (forces) in all three direction, $\sigma_{rr}, \sigma_{\phi\phi}, \sigma_{zz}$ (Figure 2). Due to symmetry, the only stress component that will be considered is the radial stress (σ_{rr}). Therefore the momentum equation reduces to the following:

$$\frac{\boldsymbol{d}\sigma_{rr}}{\boldsymbol{dt}} + \frac{(\sigma_{rr} - \sigma_{\phi\phi})}{\boldsymbol{r}} = 0 \tag{1.3}$$

With the assumption that the boundary condition of $\sigma_{rr} = 0$ at the vessel outer radius ($\boldsymbol{r} = \boldsymbol{r}_{outer}$), one can solve for the radial stress by integrating over the limits of the inner and outer radii as follow:

$$\begin{aligned} &\sigma_{rr}(\boldsymbol{n}) = \int_{\boldsymbol{n}}^{\boldsymbol{r}_{outer}} \frac{1}{\boldsymbol{r}}(\sigma_{rr} - \sigma_{\phi\phi})\boldsymbol{dr} \\ &\boldsymbol{r}_{inner} \le \boldsymbol{n} \le \boldsymbol{r}_{outer} \end{aligned} \tag{1.4}$$

The second boundary condition that plays a main role is at the inner radius, the internal pressure gradient is the negative of the radial stress, $\Delta \boldsymbol{p} = -\sigma_{rr}$ at $\boldsymbol{r} = \boldsymbol{r}_{inner}$, therefore:

$$\Delta p = -\sigma_{rr} = \int_{r_{inner}}^{r_{outer}} \frac{1}{r}(\sigma_{\phi\phi} - \sigma_{rr})dr \tag{1.5}$$

The vessel wall is assumed to be thin; therefore the radial stress can be neglected and the pressure gradient can be expressed as:

$$\Delta p = \frac{h}{r}\sigma_{\phi\phi}, \tag{1.6}$$

where $h = r_{outer} - r_{inner}$ is the vessel wall thickness, r is the deformed vessel radius, and $\sigma_{\phi\phi}$ is the circumferential stress. Equation (1.6) is known as 'law of Laplace' [11]. It illustrates that the pressure gradient required to distend a vessel against a given tension in the wall is inversely proportional to the radius of the vessel. In the circulation, the law indicates that, relative to atmospheric pressure, the tension required to balance a certain distending pressure decreases as the radius of the vessel decreases.

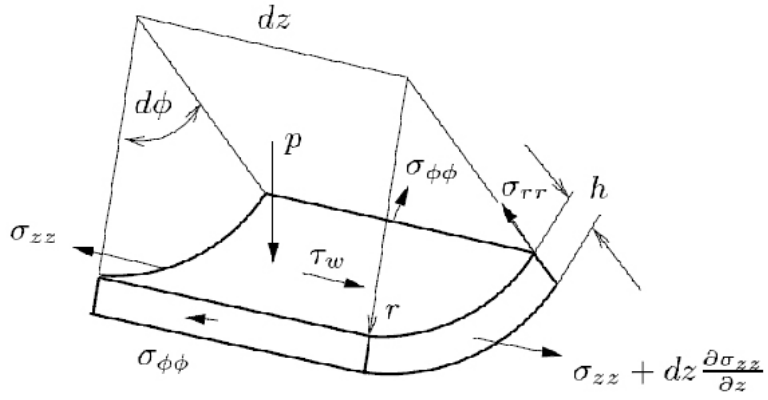

Figure 2 A Typical Arterial Wall with Three Stresses Acting on the Wall
We are considering a thin wall thickness of $h = r_{outer} - r_{inner}$, where r_{outer} is the outer radius and r_{inner} is the inner radius.

A pure elastic model can provide a valuable contribution in representing the mechanical behavior of the arterial wall and in providing a more accurate prediction for blood flow and pressure waveforms. In this study, we relate circumferential stress $\sigma_{\phi\phi}$ with radial displacement components (radial strain) using a constitutive equation as follow:

$$\sigma_{\phi\phi} = \frac{\boldsymbol{E}_{\phi\phi}}{1-\sigma_{zz}\sigma_{\phi\phi}} \frac{\Delta \boldsymbol{r}}{\boldsymbol{r_o}} \tag{1.7}$$

where,

$\frac{\Delta \boldsymbol{r}}{\boldsymbol{r_o}}$ is the radial strain

$\Delta \boldsymbol{r} = \boldsymbol{r}(\boldsymbol{z},\boldsymbol{t}) - \boldsymbol{r_o}$ is the radius difference between the deformed and undeformed radii

$\boldsymbol{r_o}$ is the undeformed radius

r is the deformed radius

$\boldsymbol{E}_{\phi\phi}$ is Young's modulus in circumferential direction

$\sigma_{zz}, \sigma_{\phi\phi}$ are Poisson ratios in circumferential and longitudinal directions

Combining Equation (1.6) and Equation (1.7) yields the following constitutive equation:

$$\Delta \boldsymbol{p} \frac{\boldsymbol{r}}{\boldsymbol{h}} = \frac{\boldsymbol{E}_{\phi\phi}}{1-\sigma_{zz}\sigma_{\phi\phi}} \frac{\Delta \boldsymbol{r}}{\boldsymbol{r_o}} \tag{1.8}$$

Setting $\sigma_{zz} = \sigma_{\phi\phi} = 0.5$ and rewriting equation (1.8) in terms of the pressure gradient, results in the following constitutive equation:

$$\Delta \boldsymbol{p} = \frac{4}{3} \frac{\boldsymbol{E}_{\phi\phi}\boldsymbol{h}}{\boldsymbol{r}} \frac{\Delta \boldsymbol{r}}{\boldsymbol{r_o}} \tag{1.9}$$

We assume that the blood vessel is initially stretched longitudinally and is inflated with the undeformed pressure, p_o. The pressure gradient $\Delta p = p(r) - p_o$ is defined as the difference between the deformed pressure, $p(r)$, and the undeformed pressure, p_o. Similarly, the pulsatile change in radius $\Delta r = r - r_o$ is defined as the difference between the deformed radius r and the undeformed radius r_o. Therefore Equation (1.9) reduces to the following:

$$p(r) - p_o = \frac{4}{3}\frac{E_{\phi\phi} h}{r_o}\frac{(r - r_o)}{r} \tag{1.10}$$

Dividing out the r term, dropping the ϕ subscript from the Circumferential Young's modulus $E_{\phi\phi}$, and rewriting equation (1.10) in terms of the deformed pressure $p(r)$, the constitutive equation becomes:

$$p(r) = \frac{4}{3}\frac{Eh}{r_o}(1 - \frac{r_o}{r}) + p_o \tag{1.11}$$

Equation (1.11) is the constitutive equation that is used in this work to describe the stress-strain relationship and the compliance of any large artery. It also includes a radius dependent modulus term (E) that was defined by Olufsen, et al [4] using an empirical decaying exponential function ($\frac{Eh}{r_o}$) shown in Figure 3 and is defined as follows:

$$\frac{Eh}{r_o} = k_1 * \exp(k_2 * r_o) + k_3 \tag{1.12}$$

where,

$$k_1 = 2x10^7\, g/(s^2 cm)$$
$$k_2 = -22.53 cm^{-1}$$
$$k_3 = 8.65x10^5\, g/(s^2 cm)$$

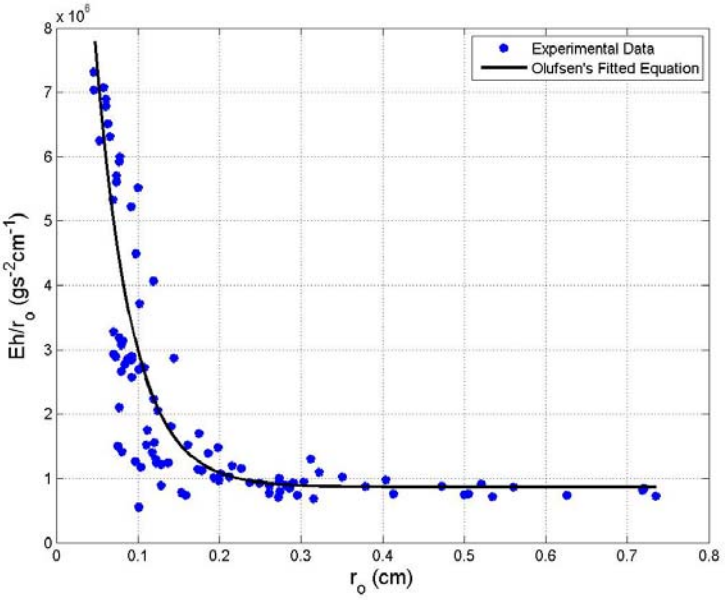

Figure 3 Radius-Dependent Young's Modulus Graph
This graph was reproduced from Olufsen, et al [4]. Young's modulus (E) times the wall thickness (h) is divided by the undeformed radius (r_o) is a function of r_o. The parameter k_1 is $2x10^7\, g/(s^2 cm)$, the parameter k_2 is $-22.53 cm^{-1}$ and the parameter k_3 is $8.65x10^5\, g/(s^2 cm)$. Note that k_3 is dominating for large vessels (ro>0.6cm) such as the aortas.

Chapter 3. Methods

3.1 Experimental Design

The goal of this research was to characterize normotensive and hypertensive aortic wall mechanics using an elastic constitutive equation. Three methods were prescribed and applied to experimental datasets of pressure-diameter cycles for aortas from normotensive and hypertensive subjects [14-20]. For all methods, internal blood pressures were computed for the corresponding experimental vessel radii. The first method approximated internal blood pressures by utilizing an elastic constitutive equation (1.11) in conjunction with Olufsen's equation (1.12). The second method approximated the internal blood pressures using equation (1.11) and (1.12); however, it used an optimized $\boldsymbol{k}_3$ parameter to best fit experimental datasets utilizing the Nelder-Mead optimization technique. The third method computed the pressure distribution using the same constitutive equation as the first two methods, however the Olufsen's equation (1.12) was not used to approximate the modulus. Instead it directly approximated the modulus from patient specific systolic and diastolic measurements using $\boldsymbol{E}_o$.

3.2 Experimental Data from Literature

Experimental internal blood pressure and aortic diameter datasets, collected from the literature, were used to derive the appropriate parameters for the constitutive equation [14-20]. Datasets included six normotensive human, two hypertensive human, and five

normotensive canine subjects. In all of the studied pressure-diameter curves, the diameter was smaller during loading (expansion) than during unloading (contraction) due to the aortic wall viscoelastic properties and accounts for each loop hysteresis. The loading region is fairly linear while the unloading region is nonlinear. This nonlinearity indicates that the vascular wall is more distensible at lower pressure than at higher pressure.

The first human study was from three Stefanadis, et al studies[14-16] where the pressure and diameter measurements were instantaneously recorded for normotensive and hypertensive thoracic aortas, using a catheter-tip micromanometer and a Y-shaped intravascular catheter (developed using sonometry in Stefanadis' laboratory) [14], respectively. In the first Stefanadis study, only three subject's pressure-diameter loops were available in this paper and were used in all three methods [14].

Figure 4.A and B show simultaneously recorded pressure-diameter loops during one cardiac cycle for two normotensive 50 year old subjects while Figure 5.A shows the hypertensive 52 year old subject. All three subjects were studied during a one day hospital stay, with a controlled room temperature of $20.0 \pm 1.0^{o}\boldsymbol{C}$. In all three cases, the pressure-diameter curve is nonlinear and reveals gradual transition from distensible to stiff behavior at higher arterial pressure. Furthermore, it exhibits hysteresis, that is, the diameter is smaller during expansion (loading) than during contraction (unloading). During loading, the aortic diameter increases quickly in early systole because of the internal pressure increase. While during diastole, diameter size is reduced in response to the drop in internal pressure. Figure 5.A also shows the increase in steepness of the 52 year old hypertensive pressure-diameter curve compared to the two 50 year old normotensive thoracic aortas displayed in Figure 4.A and B, indicating

that the thoracic aorta becomes less distensible with hypertension and vascular wall remodeling with respect to the two 50 year old normotensive patients. The second Stefanadis study [16] was of a normotensive thoracic aorta of unknown age. Figure 4.C shows the pressure-diameter loop for this normotensive subject, where a small hysteresis is present with a distensible diameter range between 2.1 to 2.3 cm and a rather low pressure range between 75 and 140 mmHg. Lastly, the third Stefanadis study [15] was of one normotensive subject and one hypertensive subject (Figure 4.C and Figure 5.B). It is interesting to note that the hysteresis curve is wider in the hypertensive thoracic aorta (Figure 5.B) than the normotensive thoracic aorta (Figure 4.C). This is mostly likely due to the aortic wall remodeling due to hypertension and exhibiting greater energy loss than the normotensive case.

Another human study was from Sonesson et al [17] for two normotensive males: a 24 year old abdominal aorta and a 69 year old abdominal aorta. The pressure measurements were collected invasively via a catheter while the inner diameter was measured non-invasively using an echo-tracking system [17]. Figure 4.E and 5.F display the two abdominal aortic pressure-diameter loops. Three important observations are seen here. First, the hysteresis curve is wider in the 69 year old male abdominal aorta than the 24 year old male abdominal aorta. This is mostly likely due to the aortic wall remodeling due to aging and exhibiting greater energy loss than the normotensive case. Second, the percentage $\Delta \boldsymbol{r}$ for the younger abdominal aorta is greater than that of an older abdominal aorta (18.5% vs. 2.3%) agreeing with the fact that the vessel wall becomes less distensible with aging hypertension. Third, the vessel diameter is larger in the older abdominal aorta than the younger abdominal

aorta (almost double in diameter size).

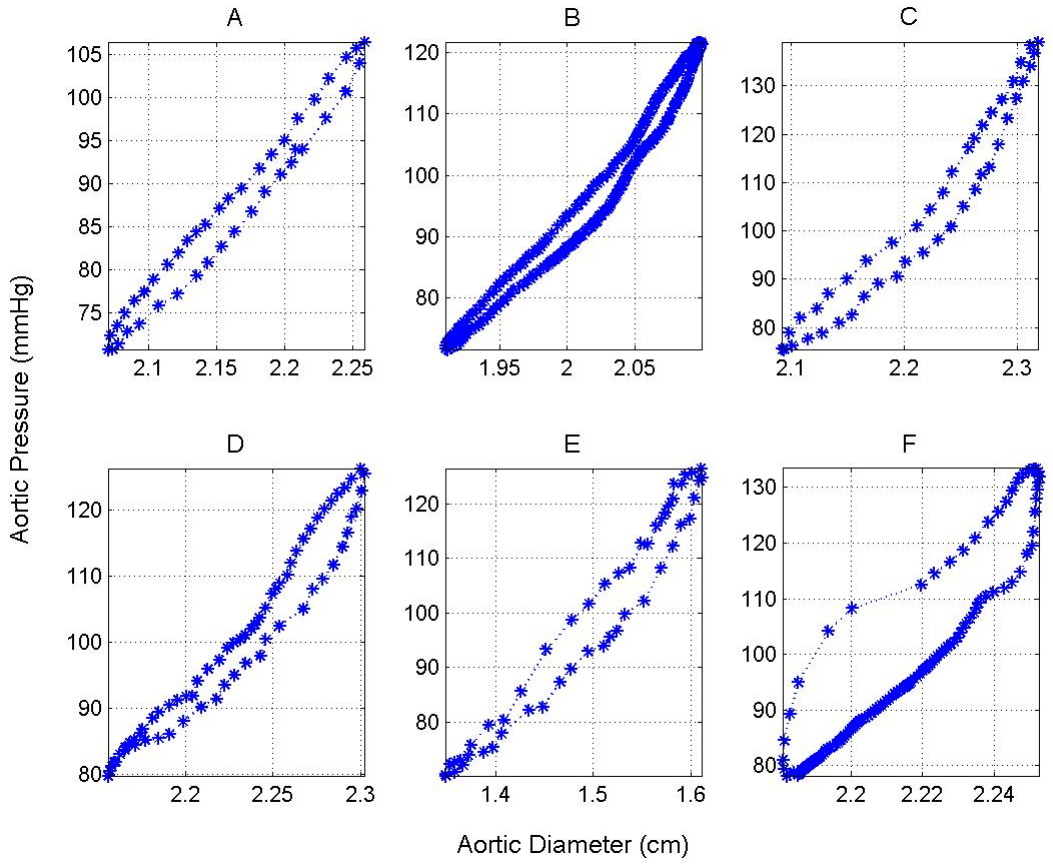

Figure 4 Human Thoracic and Abdominal Aortic Pressure-Diameter Loops
The pressure-diameter loops from Stefanadis clinical studies [14-16, 21, 22] for normotensive and hypertensive thoracic and abdominal aortas. A-D are pressure-diameter loops of thoracic aortas while E-F are pressure-diameter loops of abdominal aortas. (A) The blue loop represents a 50 year old male normotensive subject[14]. ((B) The blue pressure-diameter loop is of another normotensive 50 year old thoracic aorta [15]. (C) The blue loop is of a normotensive thoracic aorta [16]. (D) The blue loop is of a normotensive thoracic aorta [15]. (E) The blue loop is of a 24 year old male abdominal aorta [17]. (F) The blue loop is of a 69 year old male abdominal aorta [17].

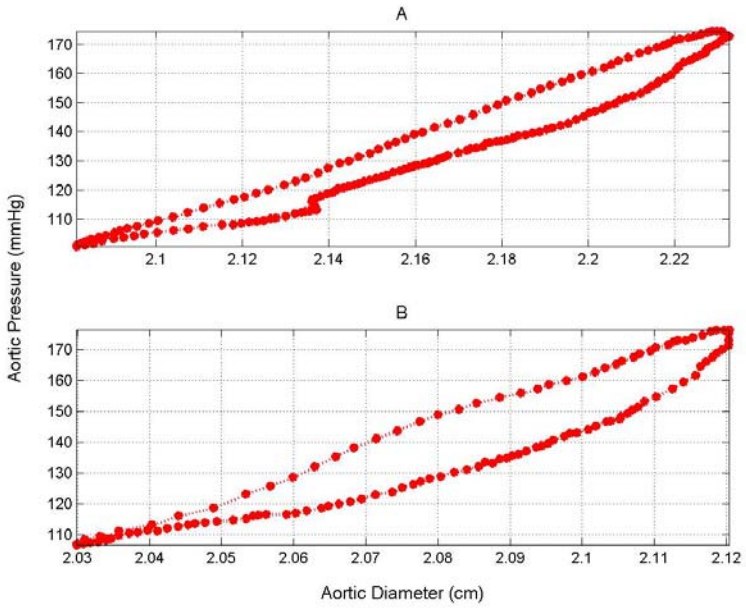

Figure 5 Hypertensive Thoracic Aortic Pressure-Diameter Loops
(A) The pressure-diameter loop from clinical study [14] for hypertensive thoracic aorta of a 52 year old. (B) The pressure-diameter loop is from Stefanadis clinical study [15] for hypertensive thoracic aorta of unknown age.

The first normotensive canine study was from Yano et al [20] for an open-chested anesthetized mongrel dog, weighing 13-20 kg. The thoracic aortic pressure was measured using micromanometer while the external diameter was measured using sonomicrometry. Figure 6.A shows the loading curve of this thoracic aorta with a diameter range between 1.3-1.6cm and pressure range between 55-130 mmHg and rather linear characteristic.

The second normotensive canine study was from Hardt et al [19]. Abdominal aortic pressure and diameter measurements were recorded from two anesthetized foxhound dogs using a pressure transducer and implanted sonomicrometer crystals, to record the diameter measurements, as seen in Figure 6.B and C.

Lastly, the third canine normotensive study was previously published in Ferguson, et al [18]. In this study, two mongrel dogs, weighing between 25-35 kg, were anesthetized and

their ascending aortic pressures were measured using micromanometer catheters and their outer diameters were recorded using ultrasonic crystal catheters. The first dog pressure-diameter loop is depicted in Figure 6.D where the dicrotic notch (end systole) is clearly seen around the diameter measurement of 2.4 cm. The second dog aortic pressure-diameter loop is displayed in Figure 6.E were the inferior vena cava (IVC) was occluded, hence the higher pressure end range.

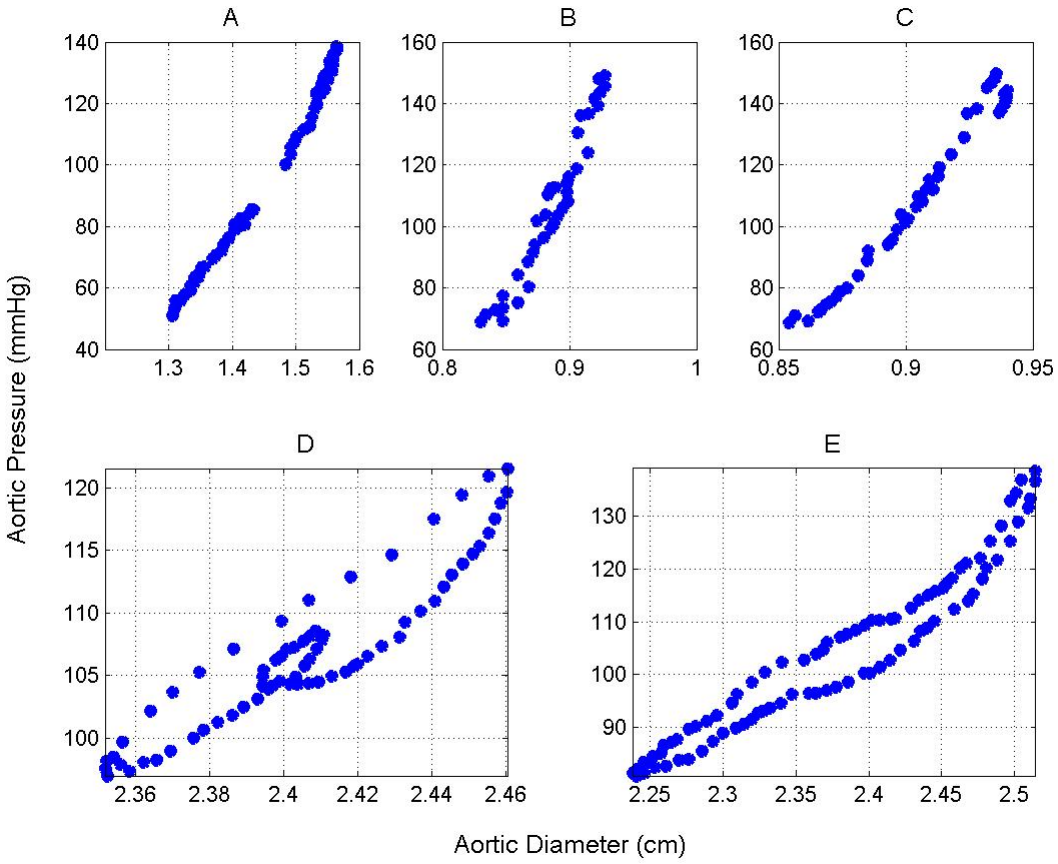

Figure 6 Thoracic, Abdominal and Ascending Aortic Dog Pressure-Diameter Curves
(A) Pressure-diameter curve from dog study [20] for a normotensive thoracic aorta. (B) Normotensive abdominal aortic pressure-diameter curve from dog study [19]. (C) Pressure-diameter curve from dog study [19] for a normotensive abdominal aorta. (D) In vivo pressure-diameter loop from dog study [18] for a normotensive ascending aorta is presented here. (E) In vivo pressure-diameter loop from dog study [18] for a normotensive ascending aorta where the IVC was occluded.

3.3 Patient-Specific Elastic Modulus E_o

For a linear elastic model, the elastic modulus can be used to predict the pressure distribution for given diameter measurements. This modulus is directly computed from the experimental dataset discussed earlier by utilizing the pulse pressure ($\Delta \boldsymbol{p}$), the diastolic

radius (r_o), and the difference between systolic and diastolic radii (Δr) as follows:

$$E_o = \frac{(\Delta P) * (r_o)}{(\Delta r)} \tag{1.13}$$

Rewriting Equation (1.13) in terms of the pressure gradient Δp yields the following:

$$\Delta p = E_o \frac{\Delta r}{r_o} \tag{1.14}$$

$$p_{\max} - p_o = E_o \frac{(r_{\max} - r_o)}{r_o} \tag{1.15}$$

Where $p_{\max}$ is the systolic pressure, p_o is the diastolic (undeformed) pressure, $r_{\max}$ is the systolic radius, and r_o is the diastolic (undeformed) radius.

Using the constitutive equation (1.10) for $r = r_{\max}$, one can derive the relationship between the elastic modulus (E_o) and Young's modulus (E) by substituting equation (1.10) into (1.15) as follow:

$$E_o \frac{(r_{\max} - r_o)}{r_o} = \frac{4}{3} \frac{Eh}{r_o} \frac{(r_{\max} - r_o)}{r_{\max}} \tag{1.16}$$

Simplifying Equation (1.16) describes the dependency of Elastic modulus on the Young's modulus as follow:

$$E_o = \frac{4}{3} \frac{Eh}{r_{\max}} \tag{1.17}$$

Therefore, the elastic constitutive equation (1.11) can be written in terms of E_o :

$$p(r) = E_o \frac{r_{\max}}{r_o}(1 - \frac{r_o}{r}) + p_o \tag{1.18}$$

Figure 7 shows the pressure-diameter loops for the six normotensive human studies for thoracic and abdominal aortas, Figure 8 displays the two hypertensive human thoracic aortas, and Figure 9 depicts the five dog normotensive studies for thoracic, ascending and abdominal aortic pressure-diameter loops. The blue doted lines are the experimental pressure-diameter curves and the straight black lines are the predicted pressures.

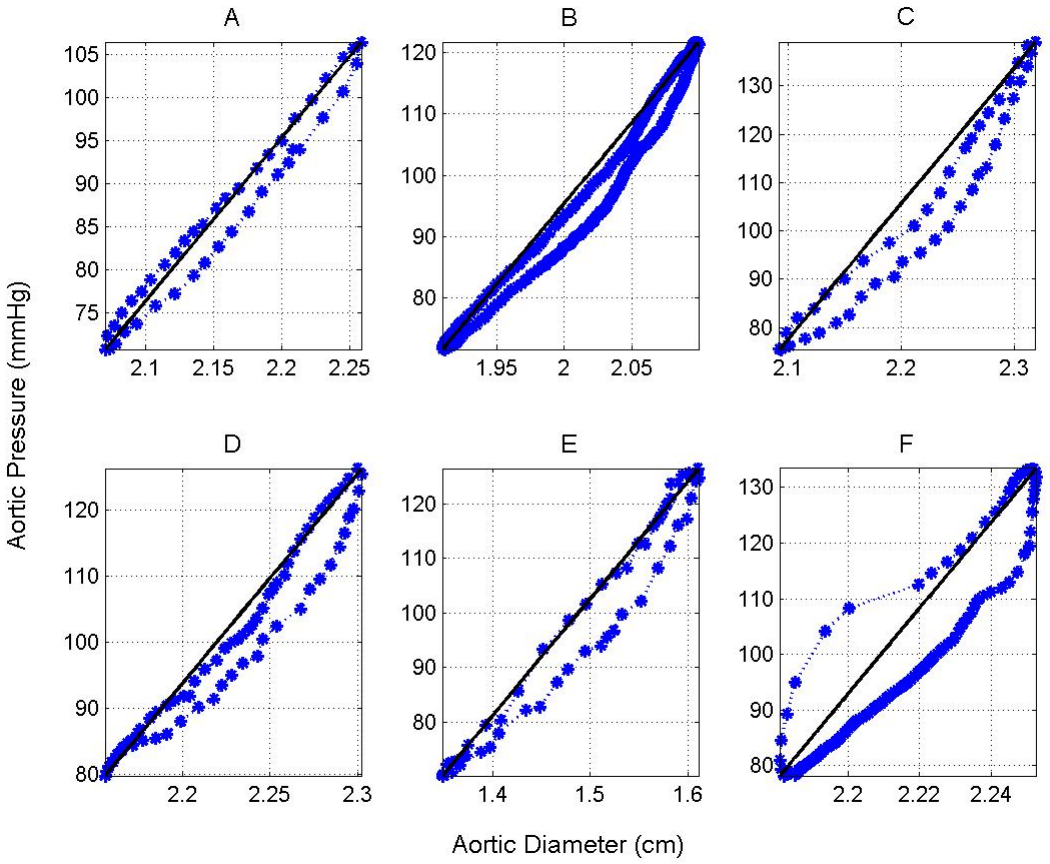

Figure 7 Normotensive Human Aortic Pressure-Diameter Loops Using Experimental E_o
(A-B) The blue pressure-diameter loops from clinical study [14] for two normotensive 50 year old normotensive thoracic aortas. The straight black lines are the constitutive equation approximations of the pressure values using E_o for all subjects. (C) The pressure-diameter loop from clinical study [16] for normotensive thoracic aorta. The blue loop represents a normotensive subject and the straight black line is the constitutive equation predicted pressure values using E_o. (D) The pressure-diameter loop from clinical study [15] for normotensive thoracic aorta. The blue loop represents a normotensive subject and the straight black line is the constitutive equation predicted pressure values using E_o. (E) In vivo pressure-diameter loop from clinical study {{; 2661 Sonesson,B. 1994; }} for a 24 year old normotensive abdominal aorta. The blue loop represents a normotensive subject and the straight black line is its constitutive equation predicted pressure values using E_o. (F) In vivo pressure-diameter loop from clinical study {{; 2661 Sonesson,B. 1994; }} for a 69 year old normotensive abdominal aorta. The blue loop represents a normotensive subject and the straight black line is its constitutive equation predicted pressure values using E_o.

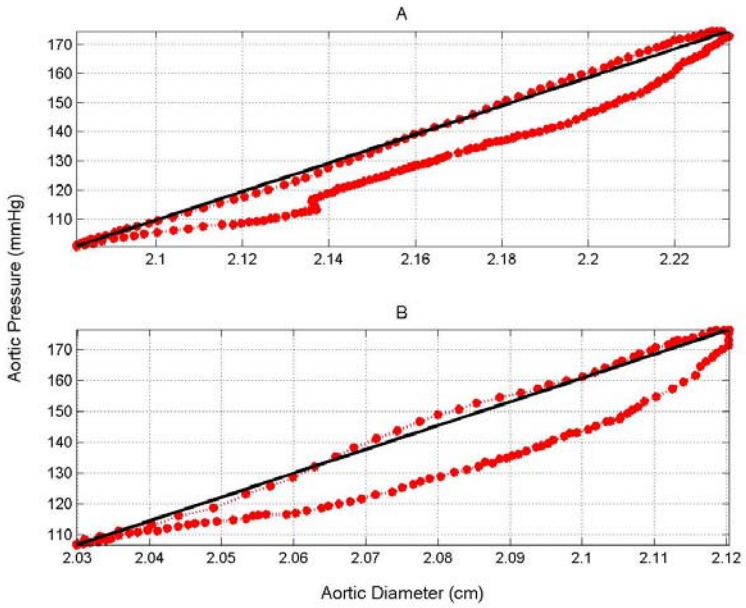

Figure 8 Hypertensive Aortic Pressure-Diameter Loops Using Experimental E_o

(A) The pressure-diameter loop from clinical study [14] for hypertensive thoracic aorta of a 52 year old. (B) The pressure-diameter loop is from another Stefanadis clinical study [15] for human hypertensive thoracic aorta. (A-B) The straight black lines are the constitutive equation approximations of the pressure values using E_o for all subjects.

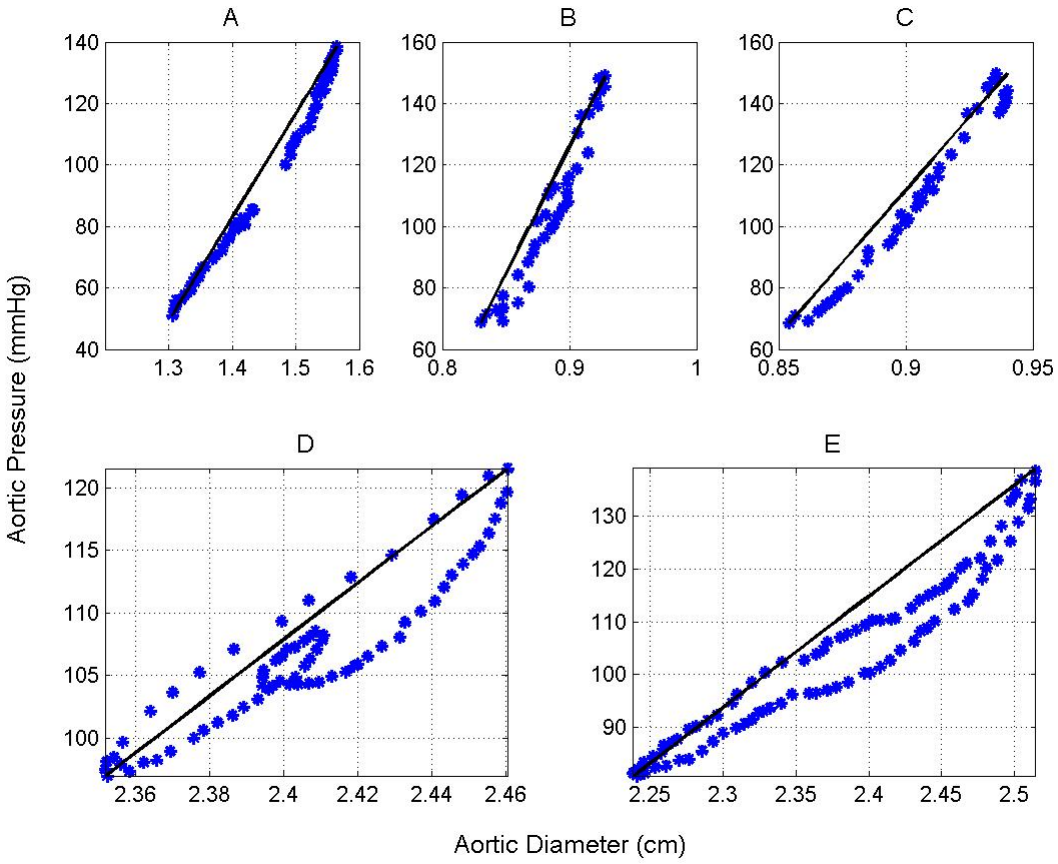

Figure 9 Normotensive Dog Aortic Pressure-Diameter Loops Using Experimental E_o

(A) In vivo pressure-diameter loop from dog study [20] for a normotensive thoracic aorta. The blue loop represents a normotensive dog and the straight black line is its constitutive equation predicted pressure values using $\boldsymbol{E}_o$. (B) In vivo pressure-diameter loop from dog study [19] for a normotensive abdominal aorta. The blue dotted curve represents a normotensive dog and the straight black line is its constitutive equation predicted pressure values using $\boldsymbol{E}_o$. (C) In vivo pressure-diameter loop from dog study [19] for a normotensive abdominal aorta. The blue loop represents a normotensive dog and the straight black line is its constitutive equation predicted pressure values using $\boldsymbol{E}_o$. (D) In vivo pressure-diameter loop from dog study [18] for a normotensive ascending aorta where the IVC was occluded. The blue loop represents a normotensive dog and the straight black line is its constitutive equation predicted pressure values using $\boldsymbol{E}_o$.

3.4 Method #1: Elastic Constitutive Equation using Olufsen's Function

The first method used Olufsen's empirical function to approximate $\frac{Eh}{r_o}$. In vivo, we assume that the undeformed radius (r_o) is the smallest possible measurement of the vessel radius, hence the diastolic radius is used as an approximation. From clinical data, $p_o, r_o,$ and r are given as inputs to the constitutive equation and the aortic pressure waveform is computed as follow:

$$p(r) = \frac{4}{3}\frac{Eh}{r_o}(1 - \frac{r_o}{r}) + p_o \tag{1.19}$$

The pressure is calculated for both normotensive and hypertensive human aortas and for normotensive canine aortas.

As seen in Figure 3, for undeformed aortic radius r_o larger than 0.6 cm equation (1.12) can be deduced to:

$$\frac{Eh}{r_o} = k_3 \tag{1.20}$$

3.5 Method #2: Elastic Constitutive Equation using Optimized k_3

In this method, an optimized version of the function $\frac{Eh}{r_o}$ was used to compute k_3 for both normotensive and hypertensive aortas. Parameters, k_1 and k_2, were not modified since they did not play a role in computing the aortic pressure for the given radii greater than 0.6 cm. The *fminsearch* function, found in the MATLAB®'s Optimization Toolbox, was used to

optimize equation (1.12) k_3 parameter. This nonlinear gradient-free method is a direct search technique that uses the concept of a simplex, or a Nelder-Mead method, to approximate the value for k_3 with tolerance of 10^{-10} (See appendix A for the MATLAB® code used to optimize the k_3 parameter for the normotensive and hypertensive datasets). The N-fold cross-validation technique was used to estimate the optimized k_3 parameter. The N-fold cross-validation is a common statistical technique that treats one dataset from N number of samples as the validation dataset, and the remaining N − 1 samples are then used as the training datasets. The cross-validation is repeated N times, with each of the N samples used once as the validation dataset. For example, for the human normotensive subjects, N is six and the cross-validation process is repeated six times, returning six optimized values for k_3.

3.6 Method #3: Elastic Constitutive Equation using an Approximation of E_o

Recall that the elastic modulus is measured directly from the pressure pulse (Δp), the diastolic radius (r_o), and the difference between systolic and diastolic radii (Δr). It is described as follows:

$$E_o = \frac{(\Delta P) * (r_o)}{(\Delta r)} \tag{1.21}$$

Rewriting Equation (1.21) in terms of the pressure gradient yields the following:

$$\Delta p = E_o \frac{\Delta r}{r_o} \tag{1.22}$$

Δp is the difference between the systolic pressure value ($p_{\max}$) and the diastolic (undeformed) pressure value (p_o) and that Δr is the difference between the systolic radius (r) and the diastolic (undeformed) radius (r_o), substituting the two terms into (1.22) leads to the following equation:

$$p_{\max} - p_o = E_o \frac{(r_{\max} - r_o)}{r_o} \tag{1.23}$$

Using equation (1.19) and equation(1.23), the elastic constitutive equation can be written in terms of E_o as follows:

$$p(r) = E_o \frac{r_{\max}}{r_o}(1 - \frac{r_o}{r}) + p_o \tag{1.24}$$

Note that the third proposed method does not require an optimization of any parameters since the overall modulus is approximated from E_o. More importantly, this method is patient specific because it uses diastolic and systolic pressure and radius measurements.

In this method, we approximate Δr to be 10% of r_o for the normotensive case [7, 9]. Finding an approximation for Δr for the hypertensive case is rather challenging, because the vessel wall mechanics varies with remodeling. However, we approximate Δr to be 6% of r_o by taking the average of the two hypertensive subjects seen in Figure 10 [14].

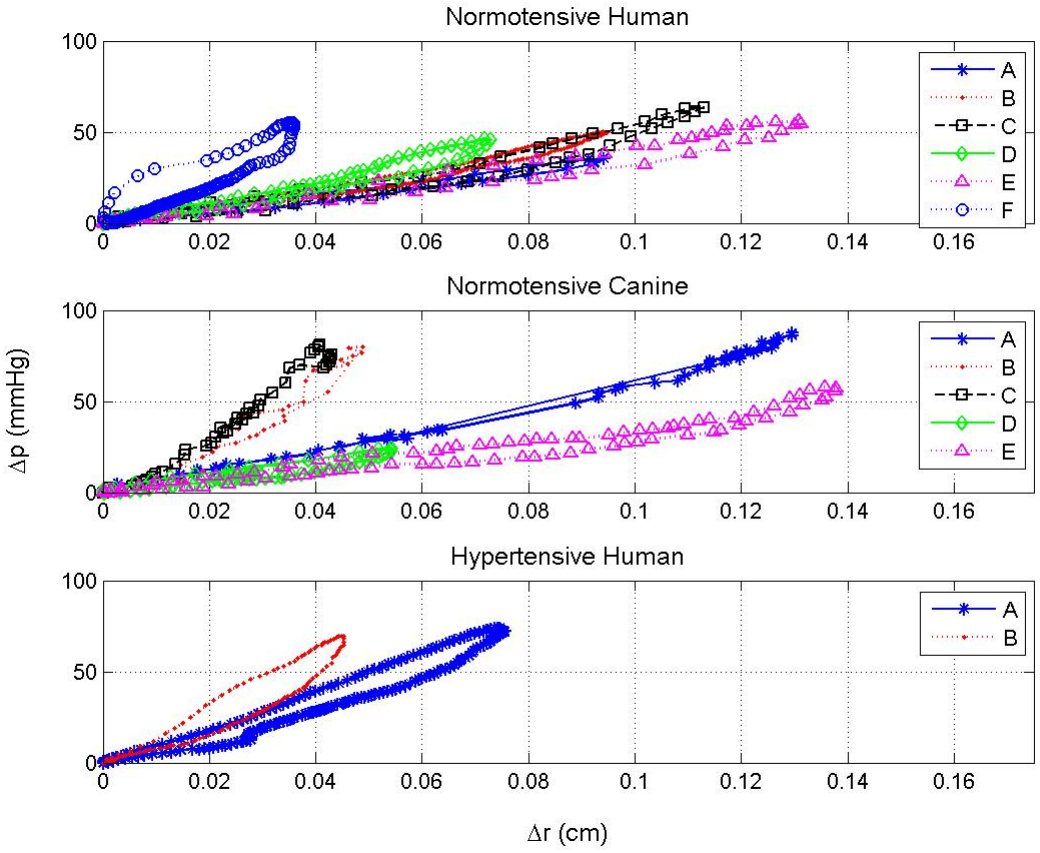

Figure 10 Change in Pressure Versus Change in Radius for All Three Cases.
In the normotensive human (subjects A-F) and canine cases (subjects A-E), found in the top two graphs, the change in radius is much greater than that of the hypertensive human case (subjects A and B), found in the bottom graph. This supports the fact that the vessel wall becomes more rigid and less distensible with hypertension, hence a smaller Δr.

3.7 Deriving k_3 Parameter from Elastic Modulus E_o

For r_o greater than 0.6cm, utilizing equation(1.20), and equation(1.17), one can derive a relationship between E_o and k_3. First, divide both sides of equation (1.20) by r_{max}:

$$\frac{\boldsymbol{k}_3}{\boldsymbol{r}_{\max}} = \frac{\boldsymbol{Eh}}{\boldsymbol{r}_{\max}} \frac{1}{\boldsymbol{r}_o} \tag{1.25}$$

Then, by rearranging equation (1.17) and substituting it into equation (1.25) the following equation is derived:

$$\frac{\boldsymbol{k}_3}{\boldsymbol{r}_{\max}} = \frac{3}{4} \frac{\boldsymbol{E}_o}{\boldsymbol{r}_o} \tag{1.26}$$

Rearranging equation (1.26) leads to the equation that relates $\boldsymbol{E}_o$ and $\boldsymbol{k}_3$ for $\boldsymbol{r}_o$ greater than 0.6cm:

$$\boldsymbol{k}_3 = \frac{3}{4} \frac{\boldsymbol{r}_{\max}}{\boldsymbol{r}_o} \boldsymbol{E}_o \tag{1.27}$$

Chapter 4. Results and Discussion

4.1 Overview of Results

Using the abovementioned methods, six human and five canine normotensive aortas were found to have mechanical properties such that the relationship between the arterial blood pressure and the internal diameter can be described by a linear constitutive model. Based on this study, using patient-specific elastic modulus E_o is a better linear representation for the normotensive human and canine aortas than the three prescribed methods. However, there is no conclusive evidence that any of the methods or the patient-specific elastic modulus E_o approach provide acceptable pressure approximations for hypertensive human aortas.

4.2 Computed Pressure-Diameter Relations for Normotensive Human Subjects

For the normotensive human case, the pressure-diameter loops of six subjects were fit using the constitutive equation previously discussed. The first four subjects were in-vivo human thoracic aortas from various Stefanadis, et al clinical studies [14-16]. While the other two studies were of abdominal normotensive human subjects [17]. Figure 11 shows all of the subject's compliance graphs, where the blue squares indicate the experimental k_3 values, the black straight lines depict the first method Eh/r_o values, the red dots display the second method k_3 results, and the green triangles represent the k_3 values using the third method.

This figure clearly shows (with the exception of the outliner, the 69 year old patient (subject F)), that the compliance curve needs to be shifted downward to better fit larger vessels such as the aorta (the remaining five subjects) $\boldsymbol{Eh}/\boldsymbol{r_o}$ value or $\boldsymbol{k_3}$ value for ($\boldsymbol{r_o} \geq 0.6\boldsymbol{cm}$).

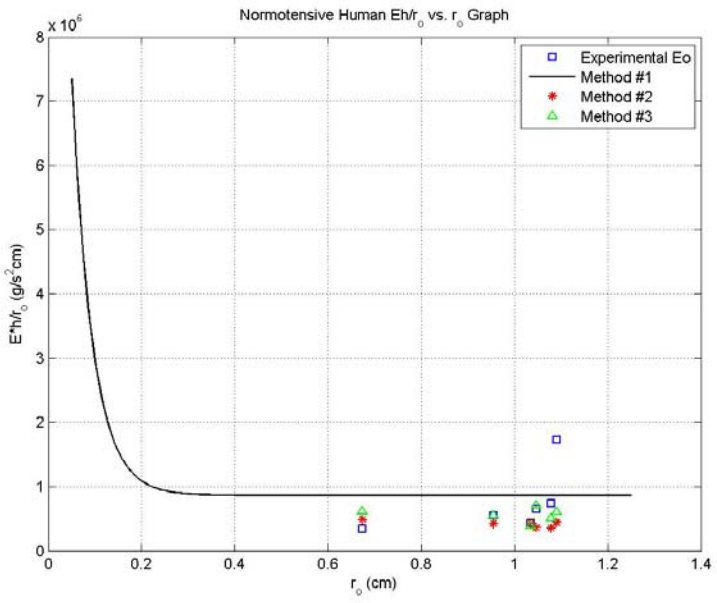

Figure 11 Modulus Graph Comparing All Methods with Experimental Normotensive Humans
This graph represents the Young's modulus ($\boldsymbol{E}$) times the wall thickness ($\boldsymbol{h}$) divided by the undeformed radius ($\boldsymbol{r_o}$) as a function of $\boldsymbol{r_o}$ for using $\boldsymbol{E_o}$ and the three prescribed methods. Experimental elastic modulus $\boldsymbol{E_o}$ approach (blue squares) is depicted here for the six normotensive human subjects. Method # 1 compliance graph is represented in the black straight line. While method #2 (red asterisk) approach and method # 3 (green triangles) approach are presented here.

Using the above compliance curve information and the internal diameter, the aortic pressures of each subject were computed by the constitutive models for all three methods and displayed in Figure 12. The blue dotted loops represent the data for normotensive human aortas. The straight lines are the constitutive equations approximations of the pressure values using the experimental $\boldsymbol{E_o}$ and all three methods. The black solid line is the computed

pressure values using experimental $\boldsymbol{E_o}$, the green line is the estimated pressure values using the first method (Olufsen's equation), the red line is the second method in predicting the pressure values using the optimized $\boldsymbol{k}_3$, and the third method (magenta line) uses the approximated $\boldsymbol{E_o}$ to compute the pressures.

It is interesting to note that in all six subjects, there is a consistent trend where there is a necking effect around pressure value of 105 ± 10 mmHg. This pattern is difficult to model with a single line, as seen in all cases. A better linear fit may be achieved using a piecewise method, where one linear line is fit to the loading linear part and the unloading portion of the curve is modeled with two different linear lines. In the unloading portion of the curve, the first part of the curve is fit to a linear line that is less steep than the curvilinear portion of the unloading pressure curve where the pressure exceeds threshold of 105 ± 10 mmHg. Also note that the slope (modulus) at this curvilinear part is higher than the loading part, in spite of the fact that the pressure is larger at unloading for the same diameter value.

As seen in Figure 12, in all six normotensive human subjects, the first method (green line) was not adequate in predicting the pressure distribution for thoracic and abdominal human aortas. Using this method resulted in overestimation of pressure values for the first five subjects (A-E) and an underestimation in pressure values for the sixth subject (F). However, the second method (red line) seem to fit two (A and B) out of the six subject's loading part of the pressure-diameter loop. It also partially fit subject C unloading part of the pressure-diameter loop and underestimated the pressure values for subject D and subject F, and overestimated the pressure values for subject E. Lastly, the third method (magenta line) fit subjects A-C loading component of the pressure-diameter loops. While this method

partially fit subject D's unloading component of the pressure-diameter loop. However, this method overestimated subject E pressure values and underestimated the pressure values for subject F. In summary, none of the three methods was an overall best fit for all subjects. However, using patient-specific modulus (black line) is the best linear line fit for the loading part of the pressure-diameter loop.

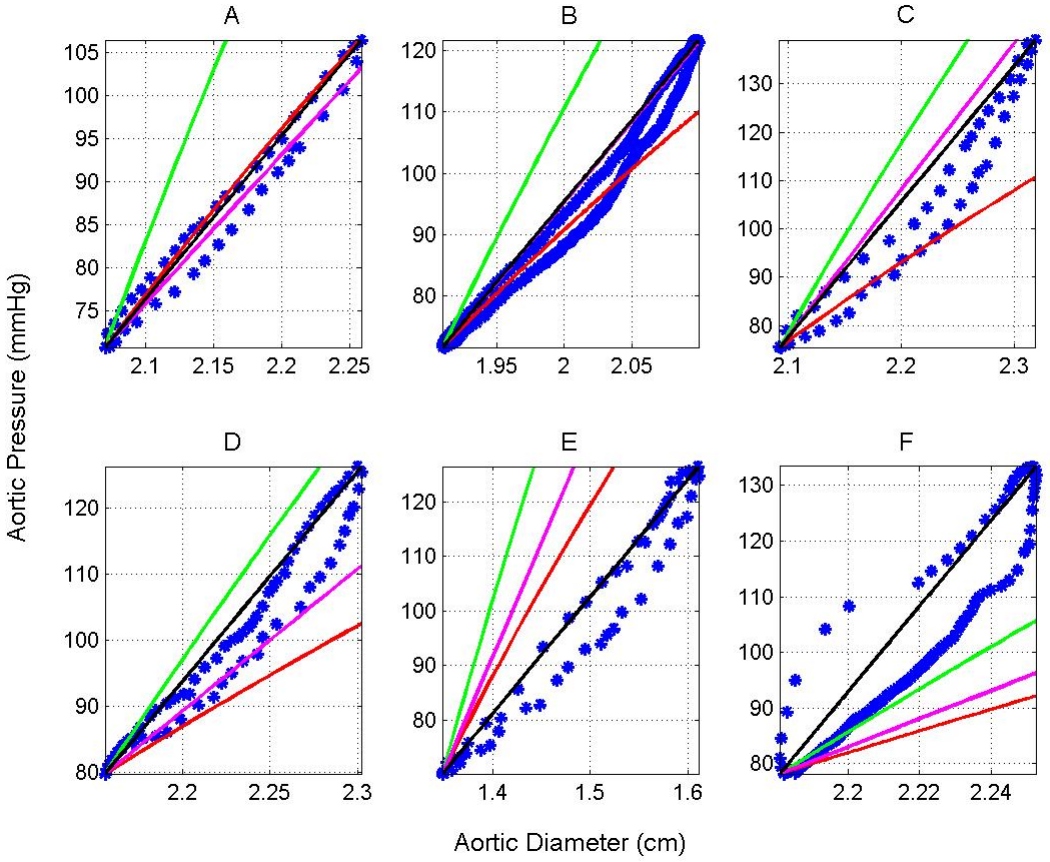

Figure 12 Thoracic and Abdominal Aortic Pressure-Diameter Loops.
The pressure-diameter loops from 6 clinical studies for normotensive thoracic and abdominal aortas [14-17, 21]. (A-D) Blue dotted loops represent the data for normotensive human thoracic aortas. (E-F) Blue dotted loops represent the data for normotensive human abdominal aortas. The straight lines are the constitutive equations approximations of the pressure values using the experimental $\boldsymbol{E}_o$, method #1 through method #3. The black solid line is the computed pressure values using experimental $\boldsymbol{E}_o$. The green line is the estimated pressure values using Method #1 (Olufsen's equation). Method #2 (red line) is the pressure values using the optimized $\boldsymbol{k}_3$. Lastly, method #3 (magenta solid line) uses the approximated $\boldsymbol{E}_o$ to compute the pressures.

Table (4.1) summarizes the computed k_3 values for the six normotensive subjects using and the patient-specific modulus (experimental E_o) and the three prescribed methods. Additionally, it displays the root mean squared error (RMSE) of the pressures in mmHg for the given range of diameters. Based on the results of the normotensive studies, the patient specific approach is the best for the human thoracic and abdominal aortas, with the smallest RMSE and patient-specific values for k_3. Tables (4.3) summarizes the six normotensive human subjects experimental E_o and the approximated E_o values using method #3.

Table 4. 1 Computed k_3 for the six normotensive human subjects

Subject	Experimental k_3	RMSE [mmHg]	Method #1 k_3	RMSE [mmHg]	Method #2 k_3	RMSE [mmHg]	Method #3 k_3	RMSE [mmHg]
A	$4.27\text{x}10^5$	2.22	$8.65\text{x}10^5$	22.35	$4.30\text{x}10^5$	2.60	$3.91\text{x}10^5$	2.11
B	$5.54\text{x}10^5$	4.57	$8.65\text{x}10^5$	23.08	$4.25\text{x}10^5$	5.46	$5.50\text{x}10^5$	4.40
C	$6.52\text{x}10^5$	8.13	$8.65\text{x}10^5$	21.07	$3.61\text{x}10^5$	13.37	$7.00\text{x}10^5$	10.69
D	$7.33\text{x}10^5$	4.29	$8.65\text{x}10^5$	8.92	$3.58\text{x}10^5$	11.51	$5.11\text{x}10^5$	6.84
E	$3.46\text{x}10^5$	5.03	$8.65\text{x}10^5$	60.33	$4.88\text{x}10^5$	19.92	$6.20\text{x}10^5$	37.38
F	$1.74\text{x}10^6$	8.29	$8.65\text{x}10^5$	11.97	$4.40\text{x}10^5$	18.99	$6.07\text{x}10^5$	16.82

Table 4. 2 r-square values for the six normotensive human aortas

Subject	Experimental r^2	Method #1 r^2	Method #2 r^2	Method #3 r^2
A	0.97	0.96	0.96	0.97
B	0.96	0.95	0.95	0.96
C	0.93	0.92	0.92	0.93
D	0.95	0.94	0.94	0.95
E	0.96	0.95	0.95	0.96
F	0.88	0.88	0.88	0.88

Table 4. 3 Computed and experimental elastic moduli for normotensive human subjects

Subject	Δr	E_o [g/(s^{2}cm)]	Method #3 Estimated Δr	Method #3 Estimated E_o [g/(s^{2}cm)]
A	0.094	$5.22\text{x}10^5$	0.104	$4.74\text{x}10^5$
B	0.095	$6.72\text{x}10^5$	0.096	$6.67\text{x}10^5$
C	0.113	$7.85\text{x}10^5$	0.105	$8.48\text{x}10^5$
D	0.073	$9.15\text{x}10^5$	0.108	$6.20\text{x}10^5$
E	0.131	$3.86\text{x}10^5$	0.067	$7.51\text{x}10^5$
F	0.036	$1.42\text{x}10^7$	0.109	$7.36\text{x}10^5$

4.3 Computed Pressure-Diameter Relations for Hypertensive Human Subjects

For the hypertensive human case, the pressure-diameter loops of two subjects were fit using the constitutive equation as discussed earlier. The first two subjects were in-vivo human thoracic aortas from Stefanadis, et al clinical studies [15, 16]. Figure 13 shows the two hypertensive subjects compliance graphs, where the blue squares indicate the experimental k_3 values, the black straight lines depict the first method Eh/r_o values, the red dots display the second method k_3 results, and the green triangles represent the k_3 values using the third method. This figure clearly shows that the compliance curve needs to be shifted upward to better fit larger vessels such as the aorta Eh/r_o value or k_3 value for ($r_o \geq 0.6cm$).

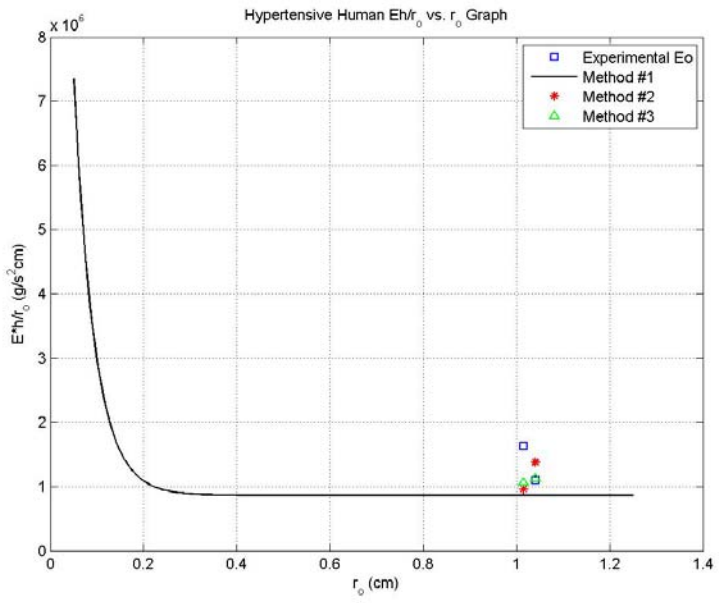

Figure 13 Modulus Graph Comparing All Methods with Hypertensive Human Datasets
This graph represents the Young's modulus ($\boldsymbol{E}$) times the wall thickness ($\boldsymbol{h}$) divided by the undeformed radius ($\boldsymbol{r_o}$) as a function of $\boldsymbol{r_o}$ for using $\boldsymbol{E_o}$ and the three prescribed methods. Experimental elastic modulus $\boldsymbol{E_o}$ approach (blue squares) is depicted here for the two hypertensive human subjects. Method # 1 compliance graph is represented in the black straight line. While method #2 (red asterisk) approach and method # 3 (green triangles) approach are present here.

Using the above compliance curve information and the internal diameter, the aortic pressures of each subject were computed by the constitutive models for all three methods and displayed in Figure 14. The blue dotted loops represent the data for hypertensive human aortas. The straight lines are the constitutive equations approximations of the pressure values using the experimental $\boldsymbol{E_o}$ and all three methods. The black solid line is the computed pressure values using experimental $\boldsymbol{E_o}$, the green line is the estimated pressure values using the first method (Olufsen's equation), the red line is the second method in predicting the pressure values using the optimized $\boldsymbol{k}_3$, and the third method (magenta line) uses the approximated $\boldsymbol{E_o}$ to compute the pressures.

As seen in Figure 14, none of the three methods was adequate in predicting the pressure distribution for the two hypertensive thoracic aortas. However, using patient-specific modulus (black line) is the best linear line fit for the loading part of the hypertensive pressure-diameter loop.

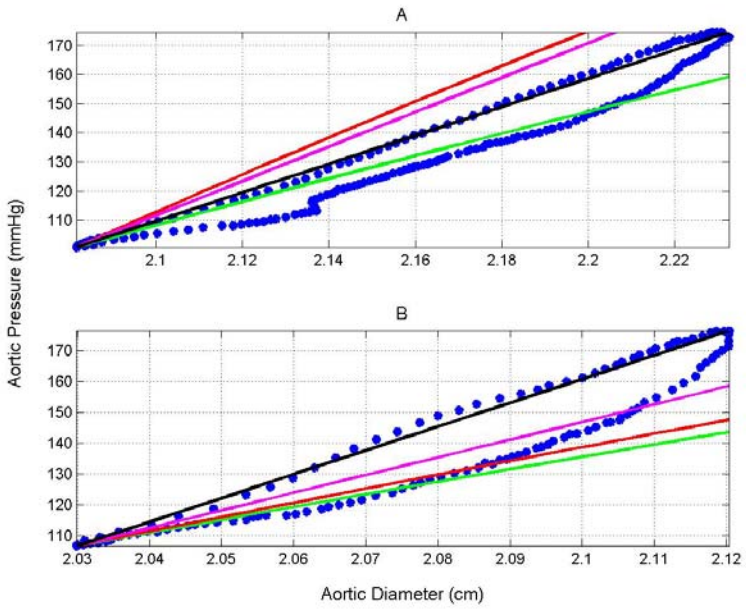

Figure 14 Hypertensive Human Thoracic Aortic Pressure-Diameter Loops.
(A) The pressure-diameter loop from clinical study [14] for hypertensive thoracic aorta of a 52 year old. (B) The pressure-diameter loop is from another Stefanadis clinical study [15] for human hypertensive thoracic aorta. (A-B) The straight lines are the constitutive equations approximations of the pressure values using $\boldsymbol{E_o}$, method #1 through method #3. The black solid line is the computed pressure values using experimental $\boldsymbol{E_o}$. The green line is the estimated pressure values using Method #1 (Olufsen's equation). Method #2 (red line) is the pressure values using the optimized $\boldsymbol{k_3}$. Lastly, method #3 uses the approximated $\boldsymbol{E_o}$ to compute the pressures as seen in the magenta solid line.

Tables (4.4) summarize the computed $\boldsymbol{k_3}$ values for the two hypertensive subjects using and the patient-specific modulus (experimental $\boldsymbol{E_o}$) and the three prescribed methods. Additionally, it displays the root mean squared error (RMSE) of the pressures in mmHg for

the given range of diameters. Table (4.6) summarizes the computed values for all two subjects using the experimental E_o and the approximation of E_o using method #3. Due to the low number of subjects in this case, no conclusive evidence was found that any of the methods or the patient-specific elastic modulus E_o approach provide acceptable pressure approximations for the two hypertensive human thoracic aortas.

Table 4. 4 Computed k_3 for the two hypertensive human subjects

Subject	Experimental k_3	RMSE [mmHg]	Method #1 k_3	RMSE [mmHg]	Method #2 k_3	RMSE [mmHg]	Method #3 k_3	RMSE [mmHg]
A	$1.09\text{x}10^6$	8.05	$8.65\text{x}10^5$	7.75	$1.38\text{x}10^6$	19.10	$1.31\text{x}10^6$	15.85
B	$1.63\text{x}10^6$	10.42	$8.65\text{x}10^5$	16.39	$9.58\text{x}10^5$	14.23	$1.23\text{x}10^6$	9.38

Table 4. 5 r-square values for the two hypertensive human aortas

Subject	Experimental r^2	Method #1 r^2	Method #2 r^2	Method #3 r^2
A	0.94	0.93	0.93	0.94
B	0.88	0.88	0.88	0.88

Table 4. 6 Computed and Experimental Elastic and Young's moduli for hypertensive subjects

Subject	Δr	E_o [g/(s^{2}cm)]	Method #3 Estimated Δr	Method #3 Estimated E_o [g/(s^{2}cm)]
A	0.045	$2.09\text{x}10^6$	0.062	$1.64\text{x}10^6$
B	0.076	$1.36\text{x}10^6$	0.061	$1.55\text{x}10^6$

4.4 Computed Pressure-Diameter Relations for Normotensive Canine Subjects

For the normotensive canine case, the pressure-diameter loops of five subjects were fit using the constitutive equation discussed in the previous section [18-20]. The first canine subject was in-vivo thoracic aorta [20], the second and third subjects were of normotensive abdominal aortas [19], and the last two subjects were of normotensive ascending aortas [18]. Figure 15 shows the five normotensive canine subjects compliance graphs, where the blue

squares indicate the experimental k_3 values, the black straight lines depict the first method Eh/r_o values, the red dots display the second method k_3 results, and the green triangles represent the k_3 values using the third method. This figure clearly shows that the compliance curve needs to be shifted slightly downward to better fit larger vessels such as the aorta Eh/r_o value or k_3 value for ($r_o \geq 0.6cm$).

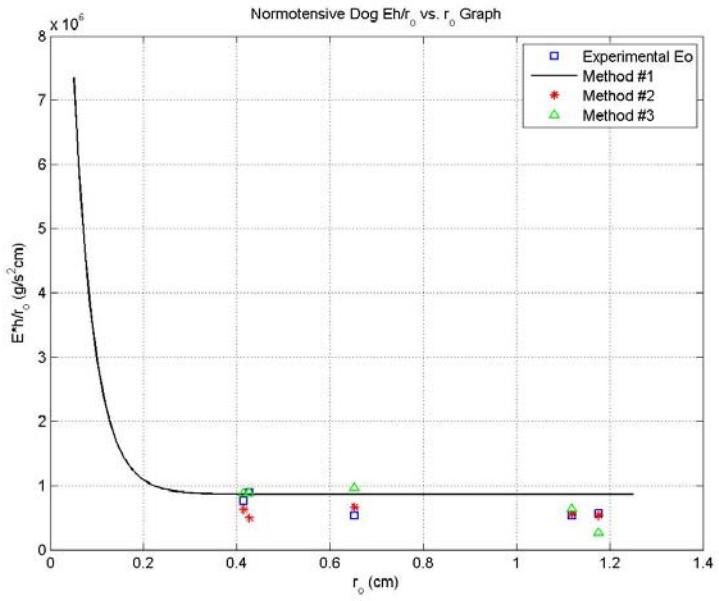

Figure 15 Modulus Graph Comparing All Methods with Normotensive Canine Datasets
This graph represents the Young's modulus (E) times the wall thickness (h) divided by the undeformed radius (r_o) as a function of r_o for using E_o and the three prescribed methods. Experimental elastic modulus E_o approach (blue squares) is depicted here for the five normotensive canine subjects. Method # 1 compliance graph is represented in the black straight line. While method #2 (red asterisk) approach and method # 3 (green triangles) approach are presented here.

Using the above compliance curve information and the internal diameter, the aortic pressures of each subject were computed by the constitutive models for all three methods and displayed in Figure 15. The blue dotted loops represent the data for normotensive canine aortas. The straight lines are the constitutive equations approximations of the pressure values using the experimental E_o and all three methods. The black solid line is the computed

pressure values using experimental $\boldsymbol{E_o}$, the green line is the estimated pressure values using the first method (Olufsen's equation), the red line is the second method in predicting the pressure values using the optimized $\boldsymbol{k}_3$, and the third method (magenta line) uses the approximated $\boldsymbol{E_o}$ to compute the pressures.

It is interesting to note that in all five subjects, there is a consistent trend where there is a necking effect at pressure value of 105 ± 10 mmHg. This pattern is difficult to model with a single line, as seen in all of the normotensive cases. As noted earlier, a better linear fit may be achieved using a piecewise method. Also note that the slope (modulus) at this curvilinear portion is higher than the loading portion, despite that the pressure is greater at unloading for the same diameter reading.

As seen in Figure 16, in all five normotensive canine subjects, the first method (green line) was adequate in predicting the pressure distribution for the loading part of the pressure-diameter loop for subject B and C. However, this method overestimated subjects A, D and E. The second method (red line) seem to fit three (B, D, and E) out of the five subject's loading part of the pressure-diameter loop. However, this method overestimated the pressure values for subject A, and underestimated the pressure values for subject C. Lastly, the third method (magenta line) fit subjects B and C loading component of the pressure-diameter loops. However, this method overestimated subjects A and E pressure values and underestimated the pressure values for subject D. In summary, none of the three methods was an overall best fit for all subjects. However, using patient-specific modulus (black line) is the best fit for the loading part of the pressure-diameter loop.

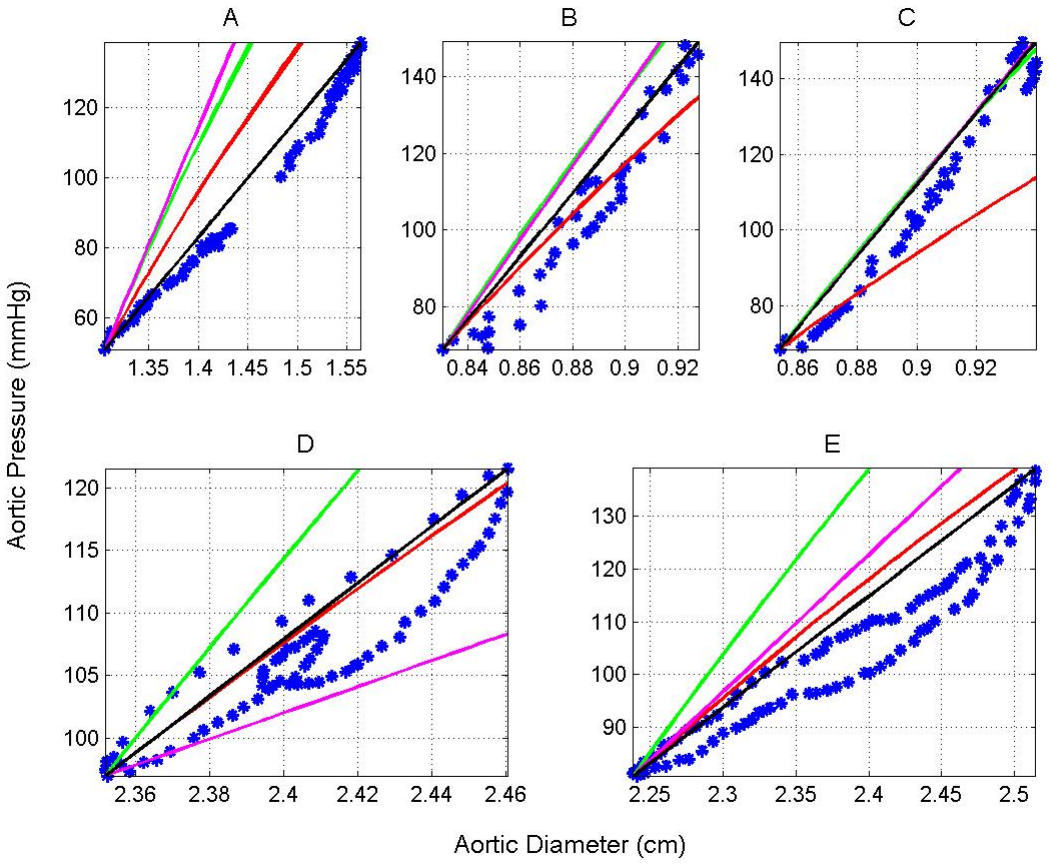

Figure 16 Thoracic, Abdominal, and Ascending Aortic Pressure-Diameter Loops.
The blue dotted pressure-diameter loop from experimental studies [18-20] for normotensive dog aortas. The straight lines are the constitutive equations approximations of the pressure values using $\boldsymbol{E}_o$, method #1 through method #3. The black solid line is the computed pressure values using experimental $\boldsymbol{E}_o$. The green line is the estimated pressure values using Method #1 (Olufsen's equation). Method #2 (red line) is the pressure values using the optimized $\boldsymbol{k}_3$. Lastly, method #3 uses the approximated $\boldsymbol{E}_o$ to compute the pressures as seen in the magenta solid line.

Table (4.7) summarizes the computed $\boldsymbol{k}_3$ values for the five normotensive canine subjects using and the patient-specific modulus (experimental $\boldsymbol{E}_o$) and the three prescribed methods. Additionally, it displays the root mean squared error (RMSE) of the pressures in mmHg for the given range of diameters. Based on the results of the normotensive canine studies, the patient specific approach is the best for thoracic, abdominal, and ascending aortas, with the smallest RMSE and patient-specific values for $\boldsymbol{k}_3$. Table (4.9) summarizes the five

normotensive canine subjects experimental E_o and the approximated E_o values using method #3.

Table 4. 7 Computed k_3 for the five normotensive dog subjects

Subject	Experimental k_3	RMSE [mmHg]	Method #1 k_3	RMSE [mmHg]	Method #2 k_3	RMSE [mmHg]	Method #3 k_3	RMSE [mmHg]
A	$5.29\text{x}10^5$	5.77	$8.65\text{x}10^5$	44.44	$6.66\text{x}10^5$	22.29	$9.62\text{x}10^5$	61.71
B	$7.61\text{x}10^5$	10.07	$8.65\text{x}10^5$	17.24	$6.24\text{x}10^5$	8.49	$8.81\text{x}10^5$	17.20
C	$8.87\text{x}10^5$	7.49	$8.65\text{x}10^5$	7.89	$4.93\text{x}10^5$	19.04	$8.93\text{x}10^5$	7.74
D	$5.57\text{x}10^5$	3.50	$8.65\text{x}10^5$	10.96	$5.31\text{x}10^5$	3.16	$2.71\text{x}10^5$	5.49
E	$5.31\text{x}10^5$	7.88	$8.65\text{x}10^5$	30.16	$5.55\text{x}10^5$	10.22	$6.20\text{x}10^5$	15.17

Table 4. 8 r-square values for the five normotensive canine aortas

Subject	Experimental r^2	Method #1 r^2	Method #2 r^2	Method #3 r^2
A	0.99	0.98	0.98	0.99
B	0.94	0.93	0.93	0.94
C	0.97	0.97	0.97	0.97
D	0.86	0.86	0.86	0.86
E	0.93	0.92	0.92	0.93

Table 4. 9 Computed and experimental Elastic and Young's moduli for normotensive canines

Subject	Δr	E_o [g/(s^{2}cm)]	Method #3 Estimated Δr	Method #3 Estimated E_o [g/(s^{2}cm)]
A	0.130	$5.88\text{x}10^5$	0.065	$1.17\text{x}10^6$
B	0.049	$6.05\text{x}10^6$	0.042	$1.07\text{x}10^6$
C	0.043	$1.07\text{x}10^6$	0.043	$1.08\text{x}10^6$
D	0.054	$7.10\text{x}10^5$	0.118	$3.28\text{x}10^5$
E	0.138	$6.30\text{x}10^5$	0.112	$7.76\text{x}10^5$

4.5 Statistical t-test for Optimized k_3 Parameter

A statistical t-test was conducted for the optimized k_3 parameter computed in the third method for the normotensive and hypertensive cases. The t distribution can be used to make significance tests for the true k_3 parameter. The null hypothesis H_0 is that the true parameter $k_3 = 8.65x10^5$. If H_0 is true, then the optimized k_3 parameter is equal to Olufsen's k_3 value of $8.65x10^5$. However, if H_0 is false, then we reject the null hypothesis and conclude that there is a significant difference in the optimized value of k_3 in comparison to Olufsen's constant value. For the each subject, the following is the summary of the Statistical Test for k_3.

$H_0 : k_3 = 8.65x10^5$ vs. $H_a : k_3 \neq 8.65x10^5$

$$T.S.: t = \frac{k_3 - 8.65x10^5}{SE}$$

$R.R.$: For $df = n - 1$ and Type I error $\alpha = 0.025$, reject H_0 if $|t| > t_{\alpha=0.025} = 1.96$

where,

H_0 is the null hypothesis

H_a is the alternative hypothesis

k_3 is the optimized parameter value

SE is the standard error of k_3

df is the degree of freedom

n is the number of iterations used for the optimization of k_3

The following table lists the t-values for the normotensive human, hypertensive human, and normotensive canine studies:

Table 4. 10 t-test values for normotensive and hypertensive subjects

Subject	$\lvert t \rvert$-Value for Normotensive Human	$\lvert t \rvert$-Value for Hypertensive Human	$\lvert t \rvert$-Value for Normotensive Canine
A	38.9329	19.0721	33.1926
B	30.4786	7.9215	27.8516
C	40.17		47.147
D	4.076		63.4128
E	29.1023		38.8005
F	6.5686		

Since all t-values are greater than 1.96, we do reject the null hypothesis that the parameter value of k_3 equals $8.65x10^5$. In other words, there is a significance difference in the optimized k_3 (method #3) value and the average k_3 value used in Olufsen's method (method #1) for the normotensive and hypertensive cases.

Chapter 5. Conclusion

5.1 Summary

Using the aforementioned methods, six human and five canine normotensive, and two hypertensive human arteries were considered to have mechanical properties such that the relationship between aortic internal pressure and diameter can be described by a linear constitutive equation. A significant reason for evaluating the parameters of a system lies in the fact that if the behavior of a system can be characterized, its parameters can be evaluated, and conversely, if a system's parameters have been evaluated its behavior can be predicted. In this work, a linear constitutive model, together with its analytical derivations, has been presented which adequately agrees with the characterization of living aortas.

The availability of the arterial pressure-diameter loops, capturing the viscoelastic characteristic of the vessels (hysteresis), are very limited and are often not readily accessible. Furthermore, in order to capture the hysteresis loop, invasive techniques are currently used to simultaneously record the patient's pressure and diameter measurements with the use of catheters, as described in the methodology section. This study shows that using the exact $\boldsymbol{E_o}$ approach does not rely on the pressure-diameter loop (invasive) but rather uses systolic and diastolic pressure and diameter values. Systolic and diastolic pressure and diameter measurements can be captured noninvasively using pressure cuff readings and radiographically (i.e. ultrasound) to measure the diameter. Therefore, the method of using the exact $\boldsymbol{E_o}$ implements a patient-specific basis using existing medical technology without exposing the patient to any additional risk or medical expenses.

This study was limited to a handful of datasets from literature. Therefore, there is a need for additional experimental datasets for multiple subjects to improve both normotensive and hypertensive models. Based on the results of this study, using the exact Elastic modulus is a better linear representation for the normotensive case. However, there is no conclusive evidence that any of the three methods that are proposed approximate the mechanical properties of normotensive or hypertensive aortas. Linking age and disease with pressure-diameter measurements is key in characterizing the mechanical properties of the arteries but it is a challenge to construct.

5.2 Future Work

In the future, we plan to expand this work by conducting large vessel studies including the thoracic aorta, the femoral arteries, and the iliac arteries. In order to collect diameter and pressure data in animal and human subjects, a small device must be designed to instantaneously measure the two variables. This device would include a micro catheter, to measure pressure, and an ultrasonic dimension gauge using piezoelectric crystals, to measure diameter changes during systole and diastole. Once this device is built, it will be tested *in vitro* using elastic tubes, *ex vivo*, *in vivo* animal studies, and lastly in human studies. By building, testing and validating this method, we hope to gain a more sophisticated understanding of normal and abnormal arterial mechanics. We believe that with a better understanding of the vascular system we will be a step closer to improving cardiovascular disease outcomes, enhancing diagnostic techniques, and advancing surgical planning.

Furthermore, we plan to implement a piecewise linear model to capture the

viscoelastic characteristics of normotensive living arteries larger than radius size of 0.6cm. As discovered in this study, there is a consistent trend in the hysteresis pressure-diameter loops of a normotensive subject, where there is a necking effect at pressure value of 105 ± 10 mmHg. As discussed earlier, this trend is difficult to model with a single linear fit (a single $\boldsymbol{k}_3$ parameter). A better linear fit may be achieved using a piecewise method, where one linear line is fit to the loading linear part and the unloading portion of the curve is modeled with two different linear lines. In the unloading portion of the curve, the first part of the curve is fit to a linear line that is less steep than the curvilinear portion of the unloading pressure curve where the pressure exceeds threshold of 105 ± 10 mmHg. By using this method, three different $\boldsymbol{k}_3$ values will be used to better prescribe the viscoelastic characteristics of large vessels using three linear fits. This proposed method requires invasive measurement of data to capture the viscoelastic characteristic of the hysteresis loading and unloading pressure-diameter loop. We predict that this approach will improve the accuracy of the pressure estimation.

REFERENCES

[1] Fung, Y.C., 1993, *Biomechanics: Mechanical Properties of Living Tissues* (New York: Springer).

[2] Holzapfel, , 2003, *Biomechanics of Soft Tissue in Cardiovascular Systems*

[3] Labropoulos, N., Ashraf Mansour, M., Kang, S.S., Oh, D.S., Buckman, J. and Baker, W.H., 2000, Viscoelastic properties of normal and atherosclerotic carotid arteries. *European journal of vascular and endovascular surgery : the official journal of the European Society for Vascular Surgery,* **19,** 221-225.

[4] Olufsen, M.S., 1999, Structured tree outflow condition for blood flow in larger systemic arteries. *The American Journal of Physiology,* **276,** H257-68.

[5] Vito, R.P. and Dixon, S.A., 2003, Blood vessel constitutive models-1995-2002. *Annual Review of Biomedical Engineering,* **5,** 413-439.

[6] Kobayashi, M., 2004, Long term outcome of femoropopliteal bypass for claudication and critical ischemia. Asian cardiovascular thoracic annals, 208.

[7] Westerhof, N., Bosman, F., De Vries, C.J. and Noordergraaf, A., 1969, Analog studies of the human systemic arterial tree. *Journal of Biomechanics,* **2,** 121-143.

[8] Segers, P., Dubois, F., De Wachter, D. and Verdonck, P., 1998, Role and relevancy of a cardiovascular simulator. *J.Cardiovasc.Eng,* **3,** 48-56.

[9] Dobrin, P.B., 1978, Mechanical properties of arterises. *Physiological Reviews,* **58,** 397-460.

[10] Westerhof, N., Bosman, F., De Vries, C.J. and Noordergraaf, A., 1969, Analog studies of the human systemic arterial tree. *Journal of Biomechanics,* **2,** 121-143.

[11] Caro, 1978, *The Mechanics of the Circulation*

[12] Li, , 2000, *The Arterial Circulation: Physical Principles and Clinical Applications*

[13] Bader, H., 1967, Dependence of wall stress in the human thoracic aorta on age and pressure. *Circulation research,* **20,** 354-361.

[14] Stefanadis, C., Dernellis, J., Vlachopoulos, C., et al, 1997, Aortic function in arterial hypertension determined by pressure-diameter relation: Effects of diltiazem. *Circulation,* **96,** 1853-1858.

[15] Stefanadis, C., Stratos, C., Vlachopoulos, C., et al, 1995, Pressure-diameter relation of the human aorta. A new method of determination by the application of a special ultrasonic dimension catheter. *Circulation,* **92,** 2210-2219.

[16] Stefanadis, C., Tsiamis, E., Vlachopoulos, C., et al, 1997, Unfavorable effect of smoking on the elastic properties of the human aorta. *Circulation,* **95,** 31-38.

[17] Sonesson, B., Lanne, T., Vernersson, E. and Hansen, F., 1994, Sex difference in the mechanical properties of the abdominal aorta in human beings. *Journal of vascular surgery : official publication, the Society for Vascular Surgery [and] International Society for Cardiovascular Surgery, North American Chapter,* **20,** 959-969.

[18] Ferguson, J.J.,3rd, Momomura, S., Sahagian, P., Miller, M.J. and McKay, R.G., 1989, The use of nitroprusside to characterize aortic pressure-diameter relationships. *Texas Heart Institute journal / from the Texas Heart Institute of St.Luke's Episcopal Hospital, Texas Children's Hospital,* **16,** 5-10.

[19] Hardt, S.E., Just, A., Bekeredjian, R., Kubler, W., Kirchheim, H.R. and Kuecherer, H.F., 1999, Aortic pressure-diameter relationship assessed by intravascular ultrasound: Experimental validation in dogs. *The American Journal of Physiology,* **276,** H1078-85.

[20] Yano, M., Kumada, T., Matsuzaki, M., et al, 1989, Effect of diltiazem on aortic pressure-diameter relationship in dogs. *The American Journal of Physiology,* **256,** H1580-7.

[21] Stalhand, J. and Klarbring, A., 2005, Aorta in vivo parameter identification using an axial force constraint. *Biomechanics and modeling in mechanobiology,* **3,** 191-199.

[22] Stalhand, J., Klarbring, A. and Karlsson, M., 2004, Towards in vivo aorta material identification and stress estimation. *Biomechanics and modeling in mechanobiology,* **2,** 169-186.

APPENDIX

Appendix A: MATLAB Code for Data Training and Optimization

1. M-File script for normotensive and hypertensive training datasets

```
%% Run all cases
%%clean up MATLAB Environment
clear all
close all
clc
%% Run the Normotensive Human Cases
%%clean up MATLAB Environment
clear global
clc
lineStyle='*';
N=6;    %Number of pressure-diameter loops Or Number of subjects
type='normotensive';
kind='Human';
dataNormoHuman = runningTrainingMethods(type, kind, N,lineStyle);
multilabel('Aortic Diameter (cm)','b',[],0.075)
multilabel('Aortic Pressure (mmHg)',[],[],0.075)
print('-djpeg', ...
    strcat('C:\Research\Thesis\simulink\NewCode\Dec4th2007\figures\', ...
    [type kind]))

%% Run the Normotensive Dog Cases
%%clean up MATLAB Environment
clear global
clc
lineStyle='*';
N=5;    %Number of pressure-diameter loops Or Number of subjects
type='normotensive';
kind='Dog'
dataNormoDog = runningTrainingMethods(type, kind, N,lineStyle);
%%%%%%%%%%%%%%%%%%%%%%%%%%%%%%%%%%%%%%%%%%%%%%%%%%%%%%%%%%%%%%%%%%%%%%%
%% plot results
%%%%%%%%%%%%%%%%%%%%%%%%%%%%%%%%%%%%%%%%%%%%%%%%%%%%%%%%%%%%%%%%%%%%%%%
figure(2)
subplot(2,2,3)
plot(dataNormoDog{4}.Experimental.diameter, ...
    dataNormoDog{4}.Experimental.RawPressure, '*', ...
        dataNormoDog{4}.Experimental.diameter, ...
        dataNormoDog{4}.Method1.pressure, 'gx:',... %Method #1 Olufsen
        dataNormoDog{4}.Experimental.diameter, ...
        dataNormoDog{4}.Method2.pressure, 'ro-',... %Method #2 Optim k3
        dataNormoDog{4}.Experimental.diameter, ...
        dataNormoDog{4}.Method3.pressure, 'ms-',... %Method #3
        dataNormoDog{4}.Experimental.diameter, ...
        dataNormoDog{4}.Experimental.pressure, 'k',... %Experimental Eo
        'LineWidth',1.5)
grid on
```

```
axis([min(dataNormoDog{4}.Experimental.diameter) ...
    max(dataNormoDog{4}.Experimental.diameter) ...
    min(dataNormoDog{4}.Experimental.RawPressure) ...
    max(dataNormoDog{4}.Experimental.RawPressure)])
title('D','Fontsize',12)
subplot(2,2,4)
plot(dataNormoDog{5}.Experimental.diameter, ...
    dataNormoDog{5}.Experimental.RawPressure, '*', ...
        dataNormoDog{5}.Experimental.diameter, ...
        dataNormoDog{5}.Method1.pressure, 'gx:',... %Method #1 Olufsen
        dataNormoDog{5}.Experimental.diameter, ...
        dataNormoDog{5}.Method2.pressure, 'ro-',... %Method #2 Optimized
k3
        dataNormoDog{5}.Experimental.diameter, ...
        dataNormoDog{5}.Method3.pressure, 'ms-',... %Method #3
        dataNormoDog{5}.Experimental.diameter, ...
        dataNormoDog{5}.Experimental.pressure, 'k', ... %Experimental Eo
        'LineWidth',1.5)
grid on
axis([min(dataNormoDog{5}.Experimental.diameter) ...
    max(dataNormoDog{5}.Experimental.diameter) ...
    min(dataNormoDog{5}.Experimental.RawPressure) ...
    max(dataNormoDog{5}.Experimental.RawPressure)])
title('E','Fontsize',12)
multilabel('Aortic Diameter (cm)','b',[],0.075)
multilabel('Aortic Pressure (mmHg)',[],[],0.075)
print('-djpeg', ...
    strcat('C:\Research\Thesis\simulink\NewCode\Dec4th2007\figures\', ...
    [type kind]))
%% Run the Hypertensive Human Cases
%%clean up MATLAB Environment
clear global
clc
lineStyle='*';
N=2;    %Number of pressure-diameter loops Or Number of subjects
type='hypertensive';
kind='Human';
dataHyperHuman = runningTrainingMethods(type, kind, N,lineStyle);
```

```
%%%%%%%%%%%%%%%%%%%%%%%%%%%%%%%%%%%%%%%%%%%%%%%%%%%%%%%%%%%%%%%%%%%%%%%
%% plot results
%%%%%%%%%%%%%%%%%%%%%%%%%%%%%%%%%%%%%%%%%%%%%%%%%%%%%%%%%%%%%%%%%%%%%%%
figure(3)
subplot(2,1,1)
plot(dataHyperHuman{1}.Experimental.diameter, ...
    dataHyperHuman{1}.Experimental.RawPressure, '*', ...
        dataHyperHuman{1}.Experimental.diameter, ...
        dataHyperHuman{1}.Method1.pressure, 'g',... %Method #1 Olufsen k3
        dataHyperHuman{1}.Experimental.diameter, ...
        dataHyperHuman{1}.Method2.pressure, 'r-', ... %Method #2 Optim k3
        dataHyperHuman{1}.Experimental.diameter, ...
        dataHyperHuman{1}.Method3.pressure, 'm-', ... %Method #3
        dataHyperHuman{1}.Experimental.diameter, ...
        dataHyperHuman{1}.Experimental.pressure, 'k', ...  %Experimenal Eo
        'LineWidth',1.95)
grid on
axis([min(dataHyperHuman{1}.Experimental.diameter) ...
    max(dataHyperHuman{1}.Experimental.diameter) ...
    min(dataHyperHuman{1}.Experimental.RawPressure) ...
    max(dataHyperHuman{1}.Experimental.RawPressure)])
title('A','Fontsize',12)
subplot(2,1,2)
plot(dataHyperHuman{2}.Experimental.diameter, ...
    dataHyperHuman{2}.Experimental.RawPressure, '*', ...
        dataHyperHuman{2}.Experimental.diameter, ...
        dataHyperHuman{2}.Method1.pressure, 'g',... %Method #1 Olufsen k3
        dataHyperHuman{2}.Experimental.diameter, ...
        dataHyperHuman{2}.Method2.pressure, 'r-', ...%Method #2 Optim k3
        dataHyperHuman{2}.Experimental.diameter, ...
        dataHyperHuman{2}.Method3.pressure, 'm-', ...%Method #3
        dataHyperHuman{2}.Experimental.diameter, ...
        dataHyperHuman{2}.Experimental.pressure, 'k', ...%Experimental Eo
        'LineWidth',1.95)
grid on
axis([min(dataHyperHuman{2}.Experimental.diameter) ...
    max(dataHyperHuman{2}.Experimental.diameter) ...
    min(dataHyperHuman{2}.Experimental.RawPressure) ...
    max(dataHyperHuman{2}.Experimental.RawPressure)])
title('B','Fontsize',12)
multilabel('Aortic Diameter (cm)','b',[],0.075)
multilabel('Aortic Pressure (mmHg)',[],[],0.075)
print('-djpeg', ...
    strcat('C:\Research\Thesis\simulink\NewCode\Dec4th2007\figures\', ...
    [type kind]))
```

2. M-File Function for normotensive and hypertensive training datasets

```
function data = runningTrainingMethods(type, kind, N, lineStyle)
%% Run training data (starting point)
global typeKind index N dirName
% N=7;
% type='normotensive';
% kind='Human';
typeKind=strcat(type, kind); %i.e. normotensiveHuman
dirSubName=strcat('c:\research\thesis\simulink\NewCode\Dec4th2007\', ...
    type, '\', kind);
dirName=strcat(dirSubName, '\dataset');
%% Load Diameter and Pressure data for Aorta
figure
alphas={'A','B','C','D','E','F','G','H'};
for index=1:N;
    load(strcat(dirName, num2str(index), '\', typeKind))
    variable=eval(typeKind);
    diameter=variable(:,1)/10;  %[cm]
    pressure=variable(:,2);   %[mmHg]
    %Return the computed pressures for all methods along with approximated
    %Eo and the new k3 value.
    eval(['data{', num2str(index), ...
        '}= trainingMethods(diameter, pressure, type, kind);'])
    %%%%%%%%%%%%%%%%%%%%%%%%%%%%%%%%%%%%%%%%%%%%%%%%%%%%%%%%%%%%%%%%
    %% plot results
    %%%%%%%%%%%%%%%%%%%%%%%%%%%%%%%%%%%%%%%%%%%%%%%%%%%%%%%%%%%%%%%%

    subplot(2,3,index)
    plot(diameter,pressure, lineStyle, ...   %Normo experimental data
        diameter,data{index}.Method1.pressure, 'gx:', ... %Method #1
        diameter,data{index}.Method2.pressure, 'ro-', ... %Method #2
        diameter,data{index}.Method3.pressure, 'ms-', ... %Method #3
        diameter,data{index}.Experimental.pressure, 'k', ... %Exp. Eo
        'LineWidth',1.5)
    grid on
    title(alphas{index},'Fontsize',12)
    axis([min(diameter) max(diameter) min(pressure) max(pressure)])
end
%% Write into an excel spreadsheet
% xlswrite(dirSubName, data{1}, [type kind])
```

3. M-File Function for normotensive and hypertensive training methods

```
function [data]=trainingMethods(diameter, actualPressuremmHg, type, kind)
%Applies the 4 methods discussed below to normotensive and hypertensive
%training datasets and also optimzes k3 for method 2.
%
% Method #1:  uses Olufsen's equation with defined k1,k2,k3 parameters:
%                       ro = min(r)
%                       Eh/ro=k1*exp(k2*ro)+k3;
%                       k1=2.00e7, k2=-22.53, k3=8.65e5
%                       p(t)=(4/3)*(Eh/ro)*(1-(ro/r)) + po
% Method #2:  uses above equations and k1 and k2 defined in method #1
%             using a new optimized value for k3
%             for both nomotensive and hypertensive:
%
%  Method #3   Uses both equations for Ep and p(t) however,
%              it approximates deltaR to be 10% of rMax, therefore ro
%              is also approximated as follow:
%                       Rmax = (1+%)ro
%
% Experimental E, use Ep to approximate (4/3)*(Eh/ro):
%                       rMax = max(r)
%                       deltaR=(rMax-ro)
%                       Ep=((pMax - po)*ro)/deltaR
%                       p(t) = Ep*(1-(ro/r)) + po
%
%       Returns a structure call DATA with all of the pressures, moduli,
%       k3s, deltaP, deltaR and RMSE for all 3 methods and experimental
%       data

%Setting up pressure to be in the right units
data.Experimental.RawPressure=actualPressuremmHg;
pressure=actualPressuremmHg*1.3332*10^3;   %Convert [mmHg] to [g/(s^2cm)]
data.Experimental.diameter=diameter;
r=diameter/2;   % deformed radii [cm]
ro=min(r);      % undeformed radius [cm] at diastolic pressure
rSystolic=max(r);    % radius [cm] at systolic pressure
Po=min(pressure);          %Diastolic pressure
pSystolic=max(pressure);   %Systolic pressure
data.Experimental.deltaP=pSystolic-Po;       %Pressure gradient
rSystolic=max(r);          %Systolic radius
data.Experimental.deltaR=rSystolic-ro;       %radius difference
h=0.12*ro;                 %Assume thickness is 12% of diastolic radius

%%%%%%%%%%%%%%%%%%%%%%%%%%%%%%%%%%%%%%%%%%%%%%%%%%%%%%%%%%%%%%%%%%%%%%%%%%%%
%uses Ep to approximate (4/3)*(Eh/ro):                                  %
%                       rSystolic = max(r)                              %
%                       deltaR=(rSystolic-ro)                           %
%                       Ep=((pMax - po)*ro)/deltaR                      %
%                       p(t) = Ep*(1-(ro/r)) + po                       %
%%%%%%%%%%%%%%%%%%%%%%%%%%%%%%%%%%%%%%%%%%%%%%%%%%%%%%%%%%%%%%%%%%%%%%%%%%%%
```

```
data.Experimental.Eo = ...  %Peterson's modulus aka elastic modulus
    (data.Experimental.deltaP*ro)/data.Experimental.deltaR;
computedPressureEo=(data.Experimental.Eo).*((r./ro)-1)+Po;
%convert to mmHg
data.Experimental.pressure=computedPressureEo/(1.3332*10^3);

%Approximate Eh/ro to compare to Compliance curve
approximatedEh_ro = mean((3/4)*(r./ro)*data.Experimental.Eo);
data.Experimental.E=approximatedEh_ro*(ro/h);  %Young's Modulus
data.Experimental.RMSE = ...
    sqrt(mean((actualPressuremmHg-data.Experimental.pressure).^2));
data.Experimental.k3 = (3/4)*rSystolic/ro*data.Experimental.Eo;

%%%%%%%%%%%%%%%%%%%%%%%%%%%%%%%%%%%%%%%%%%%%%%%%%%%%%%%%%%%%%%%%%%%%%%%%%%%%
%Method #1:  uses Olufsen's equation with defined k1,k2,k3 parameters: %
%                       Eh/ro=k1*exp(k2*ro)+k3;                          %
%                       k1=2.00e7, k2=-22.53, k3=8.65e5                  %
%                       p(t)=(4/3)*(Eh/ro)*(1-(ro/r)) + po               %
%%%%%%%%%%%%%%%%%%%%%%%%%%%%%%%%%%%%%%%%%%%%%%%%%%%%%%%%%%%%%%%%%%%%%%%%%%%%

k1=2*10^7;
k2=-22.53;
data.Method1.k3=8.65*10^5;
Eh_ro=k1*exp(k2*ro)+data.Method1.k3; %[g/s^2cm]
computedPressureOlufsen = (4/3)*(Eh_ro).*(1-(ro./r))+ Po;  %[g/(s^2cm)]
%convert to mmHg
data.Method1.pressure=computedPressureOlufsen/(1.3332*10^3);
data.Method1.E=Eh_ro*(ro/h);  %Young's Modulus from Method1
data.Method1.RMSE=sqrt(mean((actualPressuremmHg-
data.Method1.pressure).^2));



%%%%%%%%%%%%%%%%%%%%%%%%%%%%%%%%%%%%%%%%%%%%%%%%%%%%%%%%%%%%%%%%%%%%%%%%%%%%
%Method #2:  uses equation with defined k1,k2,k3 parameters: %
%                       Eh/ro=k1*exp(k2*ro)+k3;                          %
%                       k1=2.00e7, k2=-22.53,                            %
%                       k3 is optimized         %
%                       p(t)=(4/3)*(Eh/ro)*(1-(ro/r)) + po               %
%%%%%%%%%%%%%%%%%%%%%%%%%%%%%%%%%%%%%%%%%%%%%%%%%%%%%%%%%%%%%%%%%%%%%%%%%%%%

k1=2*10^7;
k2=-22.53;
%Optimize k3
%Set optimization options
options=optimset('TolFun',1e-10,'TolX',1e-3,'MaxFunEvals',2e5,...
    'MaxIter',2e5);
[k3o,fMin,exitflag,output]=fminsearch('optimizeK3New',sqrt(10^6),options);
data.Method2.k3=k3o^2;  %k3
Eh_ro=k1*exp(k2*ro)+data.Method2.k3; %[g/s^2cm]
computedPressureK3New= (4/3)*(Eh_ro).*(1-(ro./r))+ Po;  %[g/(s^2cm)]
```

```
%convert to mmHg
data.Method2.pressure=computedPressureK3New/(1.3332*10^3);
data.Method2.E=Eh_ro*(ro/h);  %Young's Modulus from Method2
data.Method2.RMSE=sqrt(mean((actualPressuremmHg-
data.Method2.pressure).^2));
data.Method2.fMin=fMin;
data.Method2.output=output;
%%%%%%%%%%%%%%%%%%%%%%%%%%%%%%%%%%%%%%%%%%%%%%%%%%%%%%%%%%%%%%%%%%%%%%%%%%%%
%Method #3: approximates deltaR to be 10% of rSystolic, therefore ro   %
%                       is also approximated as follow:                %
%                       deltaR = %*rdiastolic                          %
%                                                                      %
%%%%%%%%%%%%%%%%%%%%%%%%%%%%%%%%%%%%%%%%%%%%%%%%%%%%%%%%%%%%%%%%%%%%%%%%%%%%

if strcmp(type,'normotensive')    %Normotensive
    percentage = 0.10;
elseif  strcmp(type,'hypertensive')    %Hypertensive
    percentage = 0.06;
end
rSystolic = (1+percentage)*ro;
data.Method3.deltaR=rSystolic-ro;       %radius difference
data.Method3.Eo = ...
    (data.Experimental.deltaP*ro)/data.Method3.deltaR; %Approximation of
Eo
computedPressureEpNew=(data.Method3.Eo).*((r./ro)-1)+Po;
%convert to mmHg
data.Method3.pressure=computedPressureEpNew/(1.3332*10^3);
data.Method3.avgE=mean((3/4)*(r./ro)*data.Method3.Eo)*(ro/h);
data.Method3.stdE=std((3/4)*(r./ro)*data.Method3.Eo)*(ro/h);
data.Method3.RMSE=sqrt(mean((actualPressuremmHg-
data.Method3.pressure).^2));
data.Method3.k3=(3/4)*rSystolic/ro*data.Method3.Eo;%k3 dependent on Eo
```

4. M-File Function for optimizing k_3

```
function w = optimizeK3New(inputs)
k3=inputs(1)^2;
global index typeKind N dirName
%Load Training Set:  diameter and pressure data of normotensive
%aortic patients
k1=2*10^7; k2=-22.53;
for i=1:N
    eval(['w', num2str(i), '=0;'])
end
w=0;
for i=1:N;
    %load the other datasets to train the index dataset
    if index ~= i
        load(strcat(dirName, num2str(i), '\', typeKind))
        variable=eval(typeKind);
        diameter=variable(:,1)/10;  %[cm]
        pressure=variable(:,2)*1.3332*10^3;   %[g/s^2cm]
        r=diameter/2;
        Po=min(pressure);
        ro=min(r);
        mSize=size(diameter,1);
        Eh_ro=k1*exp(k2*ro)+k3;%[g/s^2cm]
        for j=1:mSize;
            solution= (4/3)*(Eh_ro)*(1-(ro/r(j)))+Po;
            w=w+(solution-pressure(j)).^2/mSize^2;
        end
    else
        w=0;
    end
    eval(['w', num2str(i), '=w;'])
end
for i=1:N
    eval(['w=w+sum(w', num2str(i), ');'])
end
```